ILF3 Mediated BMP2 and STAT1 Transcription Is Responsible for Hyperlipidemia-Induced Arteriosclerotic Calcification

Fei Xie
Qilu Hospital of Shandong University
Zhao-yang Wang
Bin Liu
Qilu Hospital of Shandong University
Wen Qiao
Na Li
Qilu Hospital of Shandong University
Jie Cheng
Qilu Hospital of Shandong University
Ya-min Hou
Qilu Hospital of Shandong University
Xin-ying Dong
Qilu Hospital of Shandong University
Yuguo Chen
Qilu Hospital of Shandong University https://orcid.org/0000-0001-9501-2546
Ming-xiang Zhang (zhangmingxiang@sdu.edu.cn)
Qilu Hospital of Shandong University

Article

Keywords: ILF3, arteriosclerotic calcification, BMP2, STAT1, VSMC phenotypic switch, macrophage polarization

Posted Date: November 14th, 2020

DOI: https://doi.org/10.21203/rs.3.rs-102863/v1

Abstract

Calcification is common in atherosclerotic plaque and can induce vulnerability, which further leads to myocardial infarction, plaque rupture and stroke. The mechanisms of atherosclerotic calcification are poorly characterized. Interleukin enhancer binding factor 3 (ILF3) has been identified as a novel factor affecting dyslipidemia and stroke subtypes. However, the precise role of ILF3 in atherosclerotic calcification remains unclear. Here we showed that ILF3 expression is increased in calcified human aortic vascular smooth muscle cells (HAVSMCs) and calcified atherosclerotic plaque in humans and mice. We then found that hyperlipidemia increases ILF3 expression and exacerbates calcification of VSMCs and macrophages by regulating bone morphogenetic protein 2 (BMP2) and signal transducer and activator of transcription 1 (STAT1) transcription. We further explored the molecular mechanisms of ILF3 in atherosclerotic calcification and revealed that ILF3 acts on the promoter regions of BMP2 and STAT1 and mediates BMP2 upregulation and STAT1 downregulation, which promotes atherosclerotic calcification. Our results demonstrate the effect of ILF3 in atherosclerotic calcification. Inhibition of ILF3 may be a useful therapy for preventing and even reversing atherosclerotic calcification.

Introduction

Vascular calcification is a common phenomenon in many physiological and pathological diseases including aging, end-stage renal disease, diabetes mellitus and cardiovascular diseases [1, 2]. Vascular calcification can occur in different locations of the vessel wall including intima and media but exists mainly in intimal layers in atherosclerosis and can induce atherosclerotic plaque susceptibility and further lead to myocardial infarction, plaque rupture and stroke[3].

Recent studies suggested that vascular calcification is an active cell regulatory process characterized by the involvement of various cells such as vascular smooth muscle cells (VSMCs), pericytes, myofibroblasts, macrophages, vascular mesenchymal progenitors and endothelial cells[4, 5, 6, 7]. Under multiplepro-calcificstimuli, VSMCs can undergo a phenotype switch from a contractile to osteoblastic phenotype accompanied by loss of contractile markers (smooth muscle 22 alpha [SM22α], calponin and alpha smooth muscle actin [α-SMA]) and an increase in levels of bone-related genes (runt-related transcription factor 2 [Runx2], osteopontin [OPN], osteocalcin, bone morphogenetic protein 2 [BMP2], and Msx and become the main source of osteoblastic cells, which leads to vascular calcification. In addition, macrophages can undergo a phenotype shift and participate in atherosclerotic calcification [5, 8]. Because of the diversity and complexity of calcification mechanisms, ideal drugs preventing or reversing atherosclerotic calcification are unavailable. The underlying molecular mechanisms of atherosclerotic calcification still need further study.

Interleukin enhancer-binding factor 3 (ILF3), as a double-stranded RNA (dsRNA)-binding protein, combines with other proteins, mRNAs, small noncoding RNAs, and dsRNAs to regulate transcription, translation, mRNA stability and noncoding RNA biogenesis[9]. In the cardiovascular system, ILF3 can inhibit myocardial hypertrophy[10]. Also, the association between ILF3 and myocardial infarction is

affected by low-density lipoprotein (LDL) and high-density lipoprotein (HDL) cholesterol metabolism, which indicates interactions between genes[11]. Recent studies have reported insights into the possible physiological roles of ILF3 in stroke, inflammation, and dyslipidaemia, but its role in vascular calcification has not been reported.

In this study, we used human samples and murine models with conditional ILF3 knockout and overexpression in VSMCs and macrophages to explore the roles of ILF3 in atherosclerotic calcification.

Materials And Methods

Human coronary artery samples

Atherosclerotic and control epicardial coronary artery segments were from human specimens with extensive atherosclerotic disease and healthy controls. The specimens were donated by the Shandong Red Cross Society.The experiment protocols were examined and approved by the review committee of Qilu Hospital, Jinan, China(ethics approval No. KYLL-2018(KS)-233).

Animals

ILF3 conditional transgenic and knockout mice (ILF3$^{f/f}$ mice) were generated with use of CRISPR-Cas9. The VSMC-specific ILF3 knockout (ILF3$^{-/-}$/SMA^{Cre}) and overexpression (ILF3^{over}/SMA^{Cre}) mice were bred fromILF3$^{f/f}$ mice crossed with Sm22a-creERT2$^{+/-}$ mice. Macrophage-specific ILF3 knockout (ILF3$^{-/-}$/Lyz^{Cre}) and ILF3-overexpressed (ILF3^{over}/Lyz^{Cre}) mice were bred from ILF3$^{f/f}$ mice crossed with Lyz2Cre$^{+/-}$ mice. ApoE$^{-/-}$ mice from Beijing Viewsolid Biotechnology (Beijing) were crossed with the offspring of ILF3$^{-/-}$/SMA^{Cre}, ILF3^{over}/SMA^{Cre}, ILF3$^{-/-}$/Lyz^{Cre} and ILF3^{over}/Lyz^{Cre} mice to generate ApoE$^{-/-}$ILF3$^{-/-}$/SMA^{Cre}, ApoE$^{-/-}$ILF3^{over}/SMA^{Cre}, ApoE$^{-/-}$ILF3$^{-/-}$/Lyz^{Cre} and ApoE$^{-/-}$ILF3^{over}/Lyz^{Cre} mice, respectively. The genotypes were verified by PCR. The study was conducted in strict accordance with the recommendations in the Guide for the Care and Use of Laboratory Animals of the National Institutes of Health. The protocol was approved by the Institutional Animal Care and Use Committee of Shandong University (permit no.: 07006). Mice were fed a high-fat western diet (HFD) for 4 months and then sacrificed under general anesthesia with sodium pentobarbitone and with efforts to minimize suffering. Mice were weighed and organs were harvested and fixed in 4% paraformaldehyde.

Serum index levels

We collected 0.5 to 1.0 ml of blood from the left ventricle of mice at the time of tissue harvesting after 16 weeks feeding with the HFD. Serum levels of triglycerides (TG), total cholesterol (TC), blood glucose (BG), low density lipoprotein cholesterol (LDL-C), high-density lipoprotein cholesterol (HDL-C), calcium and phosphorus were measured by standard enzymatic methods with commercial kits (Roche Diagnostics, Indianapolis, IN).

Immunohistochemistry (IHC) and immunofluorescence

For immunohistochemistry, paraffin-embedded sections were deparaffinized, rehydrated, underwent antigen retrieval and treated with hydrogen peroxide in sequence. Then, sections were blocked with 10% goat serum for 30 min at 37 °C, then incubated with specific primary antibodies including anti-ILF3 (Abcam, Cat# ab92355), anti-BMP2 (Novus, Cat# NBP1-19751), anti-Vimentin (Cell Signaling Technology, Cat#5741), anti-α-SMA (Sigma, Cat# A5228), anti-inducible nitric oxide synthase (iNOS; Abcam, Cat# ab3523), anti-arginase 1 (ARG-1;Abcam, Cat# ab239731), anti-OPN (Abcam, Cat# ab8448), anti-signal transducer and activator of transcription 1 (STAT1; Cell Signaling Technology, Cat#14994), anti-Runx2 (Abcam, Cat# ab192256) and anti-monocyte + macrophage antibody 2 (MOMA-2; Abcam, Cat# ab33451) overnight at 4 °C. After being washed 3 times, slides were exposed to streptavidin (horseradish peroxidase)-biotin labeled secondary antibody (ZSJQ-BIO, China) and reacted with diaminobenzidine. Finally, we used haematoxylin to counterstain the nucleus and a Nikon Eclipse 80imicroscope with a camera (DS-Ri1; Nikon) to acquire images.

For immunofluorescence, the same operational procedures were used as for immunohistochemistry for the first day. Then sections were incubated with primary antibodies including anti-iNOS (Abcam, Cat# ab3523), anti-ARG-1 (Abcam, Cat# ab239731), anti-OPN (Abcam, Cat# ab8448) and anti-α-SMA (Sigma, Cat# A5228) and reacted with fluorescent-labeled secondary antibodies and then 4', 6-diamidino-2-phenylindole (DAPI). Images were acquired by laser-scanning confocal microscopy (LSM710, Carl Zeiss).

Oil-red O staining andSirius red staining

Briefly, frozen sections were hydrated and washed, then immersed in 0.3% Oil-red O or Sirius red stain. Then sections were counterstained with haematoxylin and visualized under a Nikon Eclipse 80 imicroscope with a camera (DS-Ri1; Nikon). Oil-red O stain was used to detect lipids and Sirius red to examine collagen in aortic root plaques. Atherosclerotic plaque instability index was computed by using the formula (Oil-red O area + MOMA-2 area)/(α-SMA area + collagen I area).

Cell culture

Human aortic vascular smooth muscle cells (HAVSMCs) were obtained from the ScienCell (Carlsbad, CA, US) and cultured in SMC medium (SMCM) including 2% fetal bovine serum (FBS), 1% SMC growth supplement (SMCGS) and 1% penicillin/streptomycin solution. Peritoneal macrophages were collected from $ApoE^{-/-}$, $ILF3^{-/-}/Lyz^{Cre}$ and $ILF3^{over}/Lyz^{Cre}$ mice as described[8]. After being injected intraperitoneally with 6% starch for 3 days, mice were euthanized by spinal dislocation. Macrophages were collected from the peritoneal cavity by perfusion with cold phosphate-buffered saline (PBS, GibcoBRL Life Technologies). Then macrophages were grown in Dulbecco's modified Eagle's medium (DMEM, Gibco) supplemented with 10% FBS (Gibco). All cells were incubated at 37 °C in a humidified atmosphere and used after passages 3–5. Cells were starved for 24 h before each experiment. For in vitro experiments, we used osteogenic medium containing 10 mM β-glycerophosphate (β-GP, Sigma) to stimulate cell calcification for 3–14 days. Cells were treated with oxidized LDL (oxLDL; 50 μg/ml) to simulate a high lipid condition.

Lentivirus (Lv) and siRNA transfection

Lentiviruses and siRNA duplex were supplied by GenePharma (Suzhou, China). Lentiviruses encoding overexpressed ILF3 (Lv-ILF3) were incubated with VSMCs or macrophages at multiplicity of infection (MOI) of 10. After 24 h, the medium containing lentiviruses was removed and replaced with fresh medium. The siRNA duplex encoding ILF3 knockout cDNA (si-ILF3) was transfected into VSMCs or macrophages by using Lipofectamine 3000 Reagent Protocol (Invitrogen, NY, USA) in Opti-medium (Gibco) for 6 h and then replaced with fresh medium. The *Homo sapiens* siRNA sequence was 5'-CCUGUGUGAGAAAUCCAUU-3'. The lentivirus NCBI reference sequence is NO. NM_001137673.

RNA-sequencing (RNA-seq)

After HAVSMCs were transfected with ILF3 siRNA, RNAs were extracted with TRIzol reagent. We used the Qubit2.0 Fluorometer (Life Technologies, USA) and Nanodrop One spectrophotometer (Thermo Fisher Scientific, USA) to check RNA concentration and quality. The total RNA integrity was determined by using an Agilent 2100 Bioanalyzer (Agilent Technologies, USA) to ensure RNA sample integrity number (RIN) > 7. The VAHTS Total RNA-seq (H/M/R) Library Prep Kit (Vazyme, China) was used to construct RNA-seq strand-specific libraries according to the manufacturer's instructions. The quantity, insert size and concentration of purified cDNA libraries were validated by using the Qubit2.0 Fluorometer and Nanodrop One spectrophotometer. Library clusters were produced by cBot and sequencing involved the Illumina NovaSeq 6000 platform (Illumina, USA). The library generation and sequencing were performed by Genechem (Shanghai). According to the results of RNA-seq, Gene Ontology (GO) analysis and KEGG pathway analysis were used to identify cardiovascular systemic diseases and calcification-related signaling pathways.

Cellular immunofluorescence

After treatment, cells were fixed in 4% paraformaldehyde for 10 min and washed with PBS for 3 times. Then, cells were punched with 0.1% Triton X100 and blocked with 10% goat serum for 40 min at 37 °C. Cells were incubated with the primary antibodies anti-STAT1 (Cell Signaling Technology, Cat#14994) and anti-Runx2 (Abcam, Cat# ab76956) overnight at 4 °C. The second day, cells were reacted with fluorescent-labeled secondary antibodies and then 4', 6-diamidino-2-phenylindole (DAPI). Images were obtained by laser-scanning confocal microscopy (LSM710, Carl Zeiss).

Western blot analysis

Western blot analysis was conducted as previously described [8]. Membranes were incubated with primary antibodies including anti-ILF3 (Abcam, Cat# ab92355), anti-β-actin (Sigma, Cat# SAB2100037), anti-STAT1 (Cell Signaling Technology, Cat# 14994), anti-BMP2 (Abcam, Cat# ab14933), anti-Runx2 (Cell Signaling Technology, Cat# 12556), anti-Vimentin (Cell Signaling Technology, Cat# 5741), anti-iNOS (Abcam, Cat# ab178945), anti-α-SMA (Sigma, Cat# A5228), anti-OPN (Abcam, Cat# ab8448), anti-ARG-1 (Abcam, Cat# ab239731), anti-p-smad1/5 (Cell Signaling Technology, Cat# 9516) and anti-Smad1 (Cell Signaling Technology, Cat#6944). Secondary horseradish peroxidase-coupled antibodies were prepared and incubated with membranes. Images were obtained by using chemiluminescence (Millipore, Billerica, MA).

RT-PCR analysis

Total RNA was extracted from cells with TRIzol reagent and reverse-transcribed to cDNA by using HiScriptIIIRT SuperMix for qPCR (Vazyme, Nanjing, China). Quantitative RT-PCR involved using the SYBR Green Master mix kit (Roche, USA). The average cycle threshold (Ct) method was used to determine mRNA expression. The 2-ΔΔCT method was used to calculate the relative change of mRNA. The primer sequences for ILF3, BMP2, STAT1 and β-actin are in supplemental Table S1.

Alizarin-red and von Kossa staining

For Alizarin-red staining, after fixing in 4% paraformaldehyde, cells were immersed in 1% Alizarin-red solution (Solarbio, China) for 15 min. The sections of aortic root were deparaffinized and dyed with Alizarin-red for 5 min. Von Kossa staining involved using a kit (Solarbio). The cells were exposed to 5% silver nitrate solution and exposed to ultravioletray for 1 h.

Alkaline phosphatase (ALP) activity and calcium content detection

ALP activity was detected by using an ALP assay kit (Beyotime, China) and normalized to total protein concentration by the BCA Protein Assay Kit (Beyotime, China). Calcium content was determined with the Calcium Assay Kit (Nanjing Jiancheng Bioengineering Institute, China) and normalized to protein content.

Luciferase activity assay

The promoter regions of BMP2 (from the 5' region − 1360 to + 597 bp) and STAT1 (from the 5' region − 526 to + 246 bp) were ligated into the pGL3-basic vector (Cat#: E1751, Promega, WI, USA), then pGL3-BMP2-Luc and pGL3-STAT1-Luc were synthesized by digesting the plasmid with *KpnI* and *XhoI* and subcloning into the luciferase reporter vector. To further explore the binding site of ILF3 on the promoters of BMP2 and STAT1, we constructed several pGL3-BMP2-Luc reporter plasmids with progressively deleted 5'-flanking regions from the − 1360- to + 597-bp region and pGL3-STAT1-Luc reporter plasmids with progressively deleted 5'-flanking regions from the − 526- to + 246-bp region. Various lengths of the promoter region of BMP2 sequence including − 1160 to + 597, -960 to + 597, -760 to + 597, -560 to + 597, -360 to + 597, -160 to + 597, +41 to + 597, +241 to + 597 and + 425 to + 597 bp regions and STAT1 sequences including − 330 to + 246, -140 to + 246 and + 51 to + 246 bp regions were constructed. HEK293T cells were grown in 24-well plates and co-transfected with luciferase reporter plasmids and a Renilla reporter plasmid (pRL-TK, Promega) by using Lipofectamine 3000 Reagent Protocolin Opti-medium. After 24 h, firefly and renilla luciferase signals were determined by using the Dual-Luciferase reporter Assay Kit (Promega).

Chromatin immunoprecipitation assay (ChIP)

ChIP assay involved using a ChIP Assay kit (CST, USA). Nucleoprotein complexes were extracted from HAVSMCs. For immunoprecipitation, anti-ILF3 antibody (Abcam, Cat# ab131004), normal IgG antibody (CST, USA) and Histone H3 antibody (CST, USA) were used. Specific primers targeting different DNA sites

in the − 160 to + 40 bp fragment of BMP2 and the − 140 to + 50 bp fragment of STAT1 are in supplemental Table 1.

Statistical analysis

Data are presented as mean ± SEM from three replicate experiments. Student's *t* test and one-way ANOVA were used to evaluate differences between 2 groups and multiple groups, respectively, by using SPSS 18.0. Differences were considered significant at $P < 0.05$.

Results

ILF3 is upregulated in calcified atherosclerotic plaque

Mice body weight (BW) and serum levels of TC, TG, BG, HDL-C, LDL-C, calcium and phosphorus are in Supplemental Tables 2 and 3. Both VSMC-specific and macrophage-specific ILF3-knockout ApoE$^{-/-}$ILF3$^{-/-}$mice showed lower BW and TC, TG and LDL-C levels but higher HDL-C level than ApoE$^{-/-}$ mice (all $P < 0.05$). For all ILF3-overexpressed mice, BW and TC, TG and LDL-C levels were higher but HDL-C level was lower relative to ApoE$^{-/-}$ mice (*$P < 0.05$). BG, calcium and phosphorus levels did not differ between groups.

Some studies have reported that ILF3 is involved in dyslipidemia and participates in the occurrence of acute myocardial infarction[11]. To investigate the role of ILF3 in calcification of atherosclerotic plaque, we assessed whether ILF3 is increased in calcified HAVSMCs exposed to ox-LDL and in calcified atherosclerotic plaque. Calcification was induced in cultured VSMCs by treatment with osteogenic medium with or without ox-LDL for 14 days. Alizarin-red and von Kossa staining were used to find significantly increased calcium nodules in VSMCs exposed to ox-LDL (Fig. 1a). Ox-LDL–stimulated calcified VSMCs showed increased protein and mRNA levels of ILF3 as compared with controls (Fig. 1b and c). In human coronary atherosclerotic plaque, calcium nodules and ILF3 were increased in calcified plaque as compared with healthy controls (Fig. 1d). In addition, ILF3 expression was significantly increased in atherosclerotic plaque calcification inApoE$^{-/-}$ mice fed an HFD for 16 weeks (Fig. 1e). These results suggest that ILF3 plays an important role in atherosclerotic calcification.

ILF3 participates in regulating calcification gene transcription in HAVSMCs

To investigate the mechanisms of ILF3 in atherosclerosis calcification, we analyzed transcriptomic profiles in human wild-type and ILF3-deficient HAVSMCs. HAVSMCs transfected with siRNA deleting ILF3 (si-ILF3) and normal control siRNA (NC) were subjected to RNA-sEq. On differential expression analysis, inhibition of ILF3 resulted in 684 genes significantly downregulated and 940 genes significantly upregulated in HAVSMCs as compared with normal controls (Fig. 2a). High enrichment of these differentially expressed genes was associated with GO terms for processes involved in cardiovascular

systemic diseases, such as movement of endothelial cells, arterial aneurysm, aortic dilatation, apoptosis and death of cardiomyocytes and vascular lesion (Fig. 2b). KEGG pathway analysis revealed that the significantly differentially expressed genes may affect the activation of calcification-related signaling pathways including transforming growth factor-beta (TGF-β) signaling, STAT3 pathway, BMP2 signaling pathway, role of osteoblasts, osteoclasts and chondrocytes in rheumatoid arthritis and the Janus kinase (JAK)/STAT signaling pathway (Fig. 2c).

From the RNA-seq analyses and in vivo findings, we focused on the targets of calcification. The genes involved in calcification were selected to validate the dysregulated expression of mRNAs with Reads Per Kilobase of transcript, per Million mapped reads (RPKM) values > 50 identified by RNA-sEq. To further investigate the roles of ILF3 in calcification-related genes in HAVSMCs, we used hierarchical clustering based on ILF3 silence-induced change in levels of calcification-related genes. Calcification-associated genes, such as BMP2, STAT1, secreted phosphoprotein 1 (SPP1), interleukin-1 beta (IL-1β), Tissue inhibitor of metalloproteinases 2 (TIMP2) and LDL-receptor–related protein 5 (LRP5) were dysregulated (Fig. 2d). We used quantitative real-time PCR (qRT-PCR) and immunoblotting to confirm the target genes regulating calcification in ILF3-silenced HAVSMCs. Silencing ILF3 in HAVSMCs led to markedly decreased BMP2 protein level but increased STAT1 level, with the reverse for mRNA levels (Fig. 2e and f).

ILF3 promotes atherosclerotic calcification by regulating BMP2 and STAT1 gene transcription in VSMCs

To test the roles of ILF3 in atherosclerotic calcification, we first investigated the effects of ILF3 knockdown and overexpression on atherosclerotic calcification in VSMCs. ILF3 overexpression and knockdown were achieved by transduction of lentivirus (Lv-ILF3) and si-ILF3 duplex in VSMCs, respectively. Calcium deposition was estimated incultured VSMCs by using Alizarin-red and von Kossa staining. Ox-LDL stimulation increased calcium deposition in VSMCs as compared with controls, and ILF3 knockout abolished the ox-LDL effect. In addition, Lv-ILF3 overexpression induced calcification under hyperlipemia (Fig. 3a). Detection of calcium content and ALP activity showed similar trends in cultured VSMCs (Fig. 3b and 3c). Western blot analysis was used to confirm the levels of osteogenic markers including BMP2, Runx2 and STAT1 in calcified VSMCs. ILF3 knockdown reversed the ox-LDL–increased BMP2 and Runx2 levels and ox-LDL–decreased STAT1 level. In contrast, ILF3 overexpression increased BMP2 and Runx2 levels and reduced STAT1 level relative to ox-LDL alone (Fig. 3d). A BMP2-induced Smads complex is transported from cytoplasm to nucleus to increase the expression of osteogenic gene Runx2[12, 13]. Hence, we examined the change in p-smad1/5 level. ILF3 inhibition abolished the ox-LDL–induced Smad1/5 phosphorylation (Fig. 3e). In contrast, enhanced ILF3 expression increased Smad1/5 phosphorylation as compared with ox-LDL alone (Fig. 3e). In addition, Runx2 nuclear translocation is crucial for calcification of VSMCs [14, 15]. Immunofluorescence staining revealed that ox-LDL enhanced Runx2 nuclear localization but also inhibited STAT1 expression. ILF3 silencing reduced the Runx2 nuclear translocation response to ox-LDL and reversed STAT1 activity, and ILF3 overexpression had the opposite result (Fig. 3f).

To further investigate the function of ILF3 in VSMC calcification in atherosclerotic plaque, $ApoE^{-/-}$, $ApoE^{-/-}ILF3^{-/-}/SMA^{Cre}$ and $ApoE^{-/-}ILF3^{over}/SMA^{Cre}$ mice were fed an HFD for 16 weeks. As compared with $ApoE^{-/-}$ mice, $ApoE^{-/-}ILF3^{over}/SMA^{Cre}$ aortic roots showed aggravated plaque calcification, which was significantly decreased in $ApoE^{-/-}ILF3^{-/-}/SMA^{Cre}$ mice (Fig. 3g). In addition, change in levels of osteogenic markers such as BMP2, Runx2 and STAT1 in aortic roots in each group mice showed the same trend as in vitro (Fig. 3h).

ILF3 promotes atherosclerotic calcification via a VSMC phenotypic switch

A VSMC phenotypic switch from a contractile to synthetic phenotype is crucial for VSMC calcification[6]. To verify whether ILF3 enhances atherosclerotic calcification via promoting a VSMC phenotypic switch, primary HAVSMCs were cultured and treated with ox-LDL. Immunoblotting assay showed that ox-LDL induced a VSMC phenotypic switch from a contractile to synthetic phenotype by increasing levels of OPN and Vimentin (markers of VSMC synthetic phenotype) but decreasing α-SMA level (marker of VSMC contractile phenotype). ILF3 silencing significantly alleviated the VSMC phenotypic switch induced by ox-LDL (Fig. 4a). Conversely, the role of ox-LDL in the VSMC phenotypetransition was further boosted by ILF3 overexpression. Furthermore, immunofluorescence and immunohistochemical staining revealed that $ApoE^{-/-}ILF3^{-/-}/SMA^{Cre}$ mice showed lower OPN and Vimentin levels but higher α-SMA level as compared with $ApoE^{-/-}$ mice. In $ApoE^{-/-}ILF3^{over}/SMA^{Cre}$ mice, OPN and Vimentin levels were increased, but a-SMA level was downregulated (Fig. 4b and c). These results suggest that ILF3 promotes atherosclerotic calcification via a VSMC phenotypic switch.

ILF3 promotes atherosclerotic calcification by enhancing macrophage calcification and macrophage polarization

Previous study reported the role of macrophages in atherosclerotic calcification and osteogenic differentiation[8]. Next, we investigated whether ILF3 accelerates macrophage calcification in atherosclerosis. Peritoneal macrophages isolated from wild-type (WT), $ILF3^{-/-}/Lyz^{Cre}$ and $ILF3^{over}/Lyz^{Cre}$ mice were treated with or without ox-LDL. Alizarin-red and von Kossa staining showed that the knockdown of ILF3 significantly reduced calcium nodule formation in macrophages treated with ox-LDL (Fig. 5a), which was accompanied by reduced ALP activity and calcium content (Fig. 5b and c). As compared with WT macrophages incubated with ox-LDL, in ILF3-overexpressed macrophages, calcium deposition was more severe and ALP activity and calcium content were higher (Fig. 5a-c). Also, in $ILF3^{-/-}$ macrophages, the ox-LDL–induced levels of osteogenic markers BMP2 and Runx2 was markedly suppressed, but STAT1 level was concomitantly increased; ILF3 overexpression increased BMP2 and Runx2 levels and decreased STAT1 level as compared with ox-LDL alone (Fig. 5d). We also detected the effect of ILF3 on p-smad1/5 and Runx2 nuclear translocation in macrophages under hyperlipidemia. As in VSMCs, ILF3 deletion attenuated ox-LDL–induced phosphorylation of Smad1/5, but ILF3 overexpression induced Smad1/5 phosphorylation versus ox-LDL alone (Fig. 5e). Macrophagic ILF3

knockout led to decreased Runx2 nuclear translocation with ox-LDL induction and increased STAT1 level (Fig. 5f). Overexpressed ILF3 increased Runx2 nuclear translocation as compared with ox-LDL alone, with a significant decrease in STAT1 level.

To better discern whether ILF3 expedites macrophage calcification in atherosclerotic plaque, $ApoE^{-/-}$, $ApoE^{-/-}ILF3^{-/-}/Lyz^{Cre}$ and $ApoE^{-/-}ILF3^{over}/Lyz^{Cre}$ mice were fed an HFD for 16 weeks. In atherosclerotic lesions, ILF3 deletion in macrophages resulted in fewer calcium nodules together with lower expression of osteogenic markers BMP2 and Runx2 and higher STAT1 level relative to $ApoE^{-/-}$ mice (Fig. 5g and h). ILF3 overexpression in macrophages resulted in more serious calcification, higher BMP2 and Runx2 expression and reduced STAT1 level relative to ApoE-/- mice (Fig. 5g and h). Additionally, we tested the effect of macrophages on VSMC calcification. Cultured medium from ILF3-deficient macrophages was used to incubate VSMCs. VSMCs showed weaker calcification and less Runx2 level as compared with WT macrophages under ox-LDL treatment (Fig. 5i and j). Thus, ILF3 promoted macrophage calcification and participated in atherosclerotic calcification.

We next assessed whether ILF3 is involved in macrophage polarization in atherosclerotic calcification. In vitro, ox-LDL treatment increased the activity of iNOS (an M1 macrophage marker) but decreased the expression of ARG1 (an M2 macrophage marker) in WT peritoneal macrophages (Fig. 6a). However, ILF3 deletion impeded the ox-LDL–induced expression of iNOS and reversed ARG1 level. Also, ILF3 overexpression accelerated ox-LDL–induced expression of iNOS but reduced ARG1 level.

To better reveal the roles of ILF3 in macrophage polarization of atherosclerotic calcification, we evaluated the expression of iNOS and ARG1 in atherosclerotic lesions by immunofluorescence and immunohistochemistry analysis in $ApoE^{-/-}$, $ApoE^{-/-}ILF3^{-/-}/Lyz^{Cre}$ and $ApoE^{-/-}ILF3^{over}/Lyz^{Cre}$ mice. iNOS level was decreased, and ARG1 level was markedly increased in $ApoE^{-/-}ILF3^{-/-}/Lyz^{Cre}$ mice relative to $ApoE^{-/-}$mice (Fig. 6b and c). Conversely, the expression of iNOS was enhanced and that of ARG1 was reduced in $ApoE^{-/-}ILF3^{over}/Lyz^{Cre}$ versus $ApoE^{-/-}$mice (Fig. 6b and c). These results indicate that ILF3 promotes macrophages to the inflammatory M1 macrophagic phenotype in atherosclerotic calcification.

ILF3 directly binds to the BMP2 and STAT1 promoters to accelerate arteriosclerotic calcification

Studies have demonstrated that ILF3 predominantly locates in the nucleus and plays an important role in regulating transcription in mammalian cells[16, 17] either negatively or positively[18]. From the mRNA-seq results, ILF3 may promote arteriosclerotic calcification by regulating the transcription of BMP2and STAT1. To verify this hypothesis, we constructed pGL3-BMP2-Luc reporter plasmids with progressively deleted 5'-flankingregions from the − 1360- to + 597-bp region and pGL3-STAT1-Luc reporter plasmids containing progressively deleted 5'-flanking regions from the − 526- to + 246-bp region.

To confirm that ILF3 is the transcription factor of BMP2, pGL3-BMP2-Luc reporter plasmids with progressive deletions were transfected into HEK293T cells along with normal control siRNA (si-NC) or si-

ILF3. The luciferase activities of the si-ILF3 group were weakened as compared with the si-NC group, which suggests that ILF3 binds to the BMP2 promoter region (Fig. 7a). In addition, luciferase activity was significantly reduced in the upstream region + 41 to + 597 bp of the BMP2 promoter, which suggests an ILF3 binding site at -160 to + 40 bp (Fig. 7a). To further verify whether ILF3 binds to the − 160- to + 40-bp region of BMP2, ChIP assay was used with specific primers covering the promoter region − 160 to + 40 bp of BMP2. qRT-PCR results with specific primers revealed significantly elevated DNA levels that specifically bound to ILF3 as compared with negative IgG control but less to the positive H3 control (Fig. 7b and c). To further discover the binding sequences of BMP2 promoters with ILF3, we used HADDOCK software to analyze the spatial structure binding domains of the BMP2 promoter with ILF3. Figure 7d revealed that ILF3 might bind to the AGGGAG site (-53- to -48-bp fragment) of the BMP2 promoter. With the same methods, ILF3 could simultaneously bind to the GCGCCC site (-28- to -23- bp fragment) of the STAT1 promoter and regulate STAT1 transcription (Fig. 7e, f, g and h). These findings suggest that ILF3 can increase BMP2 level but decrease STAT1 level by binding to BMP2 and STAT1 promoter regions and promote arteriosclerotic calcification.

In sum, our findings illustrate the working schematic that hyperlipidemia-induced ILF3 activation mediates acceleration of atherosclerotic calcification (Fig. 8). Hyperlipidemia-increased ILF3 expression mediates BMP2 and STAT1 transcription by directly binding to their promoter regions. ILF3 upregulates BMP2 level and activates Smads signaling to elevate Runx2 transcription. Meanwhile, ILF3 suppresses STAT1 transcription, which promotes Runx2 nuclear translocation and regulates osteogenic differentiation. In addition, ILF3-mediated hyperlipidemia induces a phenotypic switch of VSMCs from contractile to a dedifferentiated synthetic phenotype and macrophages to a pro-inflammatory M1 phenotype, which in turn aggravates VSMC calcification to promote atherosclerotic calcification.

Discussion

ILF3 has been verified to play important roles in dyslipidemia and the cardiovascular system [10, 11]. However, whether ILF3 is linked to dyslipidemia-induced atherosclerotic calcification has not been reported. In the present study, we used ILF3 conditional genetic deletion and transgenic mouse models to investigate the role of ILF3 in atherosclerotic calcification. Hyperlipidemia could augment ILF3 expression in calcified VSMCs and macrophages and in atherosclerotic calcification in humans and mice. Inhibition of ILF3 blocked osteogenic differentiation in both VSMCs and macrophages under dyslipidemia. The underlying mechanisms may involve ILF3 regulating the transcription of osteogenic markers BMP2 and STAT1.

Genetic lineage-tracing studies revealed that most of the chondrocyte-like cells (98%) originate from VSMCs in atherosclerotic lesion calcification [19]. We found that knockout of ILF3 blocked osteogenic differentiation and calcium deposition in VSMCs under HFD feeding. Conversely, overexpressed ILF3 promoted atherosclerotic calcification by inducing VSMC calcification. Besides VSMCs, macrophages are involved in atherosclerotic calcification. Previous studies found that infiltrated macrophages during atherogenesis induce VSMC transdifferentiation into an osteochondrogenic phenotype by producing pro-

inflammatory cytokines and regulatory molecules, which contribute to mineral deposition in plaques [20, 21]. Co-culture studies of macrophages and VSMCs in vitro suggested that VSMC-induced Runx2 expression promotes macrophage migration and formation of osteoclast-like cells[22]. In this study, ILF3 promoted macrophage calcification in atherosclerotic calcification and isolated macrophages under dyslipidemia. Also, medium from cultured ILF3$^{-/-}$ macrophages incubated with VSMCs eliminated calcified nodules and a decrease in Runx2 expression. Our results suggest that ILF3 plays an important role in driving arteriosclerosis calcification by accelerating the osteogenic differentiation of VSMCs and macrophages.

Increasing evidence suggests that vascular calcification is an active cell-regulatory process and Runx2 is indispensable for calcification occurrence and development [4, 23, 24]. Here, we provide evidence that hyperlipidemia promotes Runx2 expression in calcified VSMCs and macrophages and atherosclerotic calcification. ILF3 deletion decreased hyperlipidemia-induced Runx2 protein content, but ILF3 overexpression increased Runx2 level concomitant with increased ALP activity.

VSMCs are non-terminally differentiated and show phenotypic plasticity, which is considered a major contribution to vascular calcification [6]. Also, a VSMC osteogenic phenotype switch facilitates intimal calcification in atherosclerotic plaque [19]. In this study, ILF3 induced a VSMC phenotype switch from a contractile to synthetic phenotype with an increase in levels of synthetic markers OPN and Vimentin and decrease in level of the contractile marker α-SMA.

The role and mechanism of macrophages in atherosclerotic calcification are still unclear. Studies reported that the pro-inflammatory M1 phenotype of macrophages is activated during atherosclerotic calcium deposition, and the pro-inflammatory atherogenic phenotype of macrophages was significantly correlated with atherosclerotic calcification[5, 25]. In our studies, hyperlipidemia activated macrophagic ILF3 and increased the level of the M1 marker iNOS and weakened that of the M2 marker ARG-1 in macrophages, which indicates that ILF3 aggravated a shift to a pro-inflammatory phenotype. Hyperlipidemia upregulated ILF3, increased Runx2 activity and promoted atherosclerotic calcification in the M1 macrophage phenotype. Moreover, medium from cultured ILF3$^{-/-}$macrophages incubated with VSMCs eliminated calcified nodules and decreased Runx2 expression, so cytokines from M1 macrophages significantly promoted the calcification of VSMCs.

Studies indicated that BMP2 and STAT1 play important roles in vascular calcification by regulating Runx2 expression[15, 26]. BMP2 induces Smad proteins phosphorylation, and activated Smads complex are transported from cytoplasm to the nucleus to increase the expression of the osteogenic gene Runx2[12, 13]. Our data showed that ILF3 increased BMP2 level and Smad1/5 phosphorylation and further upregulated Runx2 expression, so ILF3 is involved in arteriosclerotic calcification by modulating BMP2/Smads signaling. STAT1 has a negative regulatory role in Runx2-mediated osteoblast differentiation[27]. STAT1 suppresses osteoblast differentiation by interfering with Runx2 nuclear localization and transcriptional activity [15, 28, 29]. In our studies, ILF3 regulated Runx2 nuclear translocation by suppressing STAT1 activity

in VSMCs and macrophages under hyperlipidemia. In the hyperlipidemic condition, nuclear Runx2 level was increased but that of STAT1 was decreased. Inhibition of ILF3 induced STAT1 expression and Runx2 cytoplasmic translocation as compared with the hyperlipidemic condition. Furthermore, ILF3 overexpression enhanced Runx2 level in the nucleus but reduced STAT1 level under the hyperlipidemic condition. These findings demonstrate that one of the targets for ILF3 to promote atherosclerotic calcification is mediated by modulation of STAT1 transcription and thusRunx2 nuclear translocation.

Some studies have found that ILF3 can regulate transcription as a transcriptional activator [30]. In addition, DNA affinity chromatography and subsequent ChIP assays confirmed that NF90/NF110 can associate with gene regulation by binding DNA[31, 32, 33, 34, 35]. In the current study, mRNA-seq demonstrated that ILF3 genetic deficiency in VSMCs decreased BMP2 mRNA level but enhanced STAT1 level. Furthermore, we verified that ILF3 could enhance BMP2 and weaken STAT1 transcription by directly binding to their promoter regions.

In conclusion, we report the roles of ILF3 in the osteogenic switch of VSMCs and macrophages by regulating BMP2 and STAT1 transcription. ILF3 could mediate upregulation of BMP2 and suppression of STAT1 expression under hyperlipidemia to promote atherosclerotic calcification, which augmented the risk of atherosclerotic lesion instability. Inhibition of ILF3 may be a potential therapeutic target for preventing atherosclerotic calcification and lesion rupture.

Declarations

Conflict of Interest

The authors declare that they have no conflict of interest.

Acknowledgements

This work was supported by the National Natural Science Foundation of China (#91839301 and #81970251), the National key R & D program of China (#2017YFC0908700, 2017YFC0908703) and the Taishan Scholar Project of Shandong Province of China (No. ts20190972).

References

1. Abedin M, Tintut Y, Demer LL. Vascular calcification: mechanisms and clinical ramifications. *Arterioscler Thromb Vasc Biol* **24**, 1161–1170 (2004).
2. Shanahan CM, Crouthamel MH, Kapustin A, Giachelli CM. Arterial calcification in chronic kidney disease: key roles for calcium and phosphate. *Circ Res* **109**, 697–711 (2011).
3. Taylor AJ, *et al.* A comparison of the Framingham risk index, coronary artery calcification, and culprit plaque morphology in sudden cardiac death. *Circulation* **101**, 1243–1248 (2000).

4. Sun Y, *et al.* Smooth muscle cell-specific runx2 deficiency inhibits vascular calcification. *Circ Res* **111**, 543–552 (2012).
5. Fu Y, *et al.* Shift of Macrophage Phenotype Due to Cartilage Oligomeric Matrix Protein Deficiency Drives Atherosclerotic Calcification. *Circ Res* **119**, 261–276 (2016).
6. Bardeesi ASA, *et al.* A novel role of cellular interactions in vascular calcification. *J Transl Med* **15**, 95 (2017).
7. Han SH, *et al.* Relationship between coronary endothelial function and coronary calcification in early atherosclerosis. *Atherosclerosis* **209**, 197–200 (2010).
8. Li P, *et al.* Correction: Loss of PARP-1 attenuates diabetic arteriosclerotic calcification via Stat1/Runx2 axis. *Cell Death Dis* **11**, 97 (2020).
9. Castella S, Bernard R, Corno M, Fradin A, Larcher JC. Ilf3 and NF90 functions in RNA biology. *Wiley Interdiscip Rev RNA* **6**, 243–256 (2015).
10. Yang RH, Tan X, Ge LJ, Sun JC, Peng XD, Wang WZ. Interleukin enhancement binding factor 3 inhibits cardiac hypertrophy by targeting asymmetric dimethylarginine-nitric oxide. *Nitric Oxide* **93**, 44–52 (2019).
11. Yoshida T, *et al.* Association of polymorphisms of BTN2A1 and ILF3 with myocardial infarction in Japanese individuals with different lipid profiles. *Mol Med Rep* **4**, 511–518 (2011).
12. Noel D, *et al.* Short-term BMP-2 expression is sufficient for in vivo osteochondral differentiation of mesenchymal stem cells. *Stem Cells* **22**, 74–85 (2004).
13. Jonason JH, Xiao G, Zhang M, Xing L, Chen D. Post-translational Regulation of Runx2 in Bone and Cartilage. *J Dent Res* **88**, 693–703 (2009).
14. Deng L, Huang L, Sun Y, Heath JM, Wu H, Chen Y. Inhibition of FOXO1/3 promotes vascular calcification. *Arterioscler Thromb Vasc Biol* **35**, 175–183 (2015).
15. Kim S, *et al.* Stat1 functions as a cytoplasmic attenuator of Runx2 in the transcriptional program of osteoblast differentiation. *Genes Dev* **17**, 1979–1991 (2003).
16. Saunders LR, *et al.* Characterization of two evolutionarily conserved, alternatively spliced nuclear phosphoproteins, NFAR-1 and – 2, that function in mRNA processing and interact with the double-stranded RNA-dependent protein kinase, PKR. *J Biol Chem* **276**, 32300–32312 (2001).
17. Krasnoselskaya-Riz I, *et al.* Nuclear factor 90 mediates activation of the cellular antiviral expression cascade. *AIDS Res Hum Retroviruses* **18**, 591–604 (2002).
18. Reichman TW, Muniz LC, Mathews MB. The RNA binding protein nuclear factor 90 functions as both a positive and negative regulator of gene expression in mammalian cells. *Mol Cell Biol* **22**, 343–356 (2002).
19. Naik V, *et al.* Sources of cells that contribute to atherosclerotic intimal calcification: an in vivo genetic fate mapping study. *Cardiovasc Res* **94**, 545–554 (2012).
20. Callegari A, Coons ML, Ricks JL, Rosenfeld ME, Scatena M. Increased calcification in osteoprotegerin-deficient smooth muscle cells: Dependence on receptor activator of NF-kappaB

ligand and interleukin 6. *J Vasc Res* **51**, 118–131 (2014).

21. Ceneri N, *et al.* Rac2 Modulates Atherosclerotic Calcification by Regulating Macrophage Interleukin-1beta Production. *Arterioscler Thromb Vasc Biol* **37**, 328–340 (2017).
22. Byon CH, *et al.* Runx2-upregulated receptor activator of nuclear factor kappaB ligand in calcifying smooth muscle cells promotes migration and osteoclastic differentiation of macrophages. *Arterioscler Thromb Vasc Biol* **31**, 1387–1396 (2011).
23. Engelse MA, Neele JM, Bronckers AL, Pannekoek H, de Vries CJ. Vascular calcification: expression patterns of the osteoblast-specific gene core binding factor alpha-1 and the protective factor matrix gla protein in human atherogenesis. *Cardiovasc Res* **52**, 281–289 (2001).
24. Tyson KL, Reynolds JL, McNair R, Zhang Q, Weissberg PL, Shanahan CM. Osteo/chondrocytic transcription factors and their target genes exhibit distinct patterns of expression in human arterial calcification. *Arterioscler Thromb Vasc Biol* **23**, 489–494 (2003).
25. Tintut Y, Patel J, Territo M, Saini T, Parhami F, Demer LL. Monocyte/macrophage regulation of vascular calcification in vitro. *Circulation* **105**, 650–655 (2002).
26. Franceschi RT, Xiao G, Jiang D, Gopalakrishnan R, Yang S, Reith E. Multiple signaling pathways converge on the Cbfa1/Runx2 transcription factor to regulate osteoblast differentiation. *Connect Tissue Res* **44 Suppl 1**, 109–116 (2003).
27. Takayanagi H, *et al.* RANKL maintains bone homeostasis through c-Fos-dependent induction of interferon-beta. *Nature* **416**, 744–749 (2002).
28. Li J, He X, Wei W, Zhou X. MicroRNA-194 promotes osteoblast differentiation via downregulating STAT1. *Biochem Biophys Res Commun* **460**, 482–488 (2015).
29. Tajima K, *et al.* Inhibition of STAT1 accelerates bone fracture healing. *J Orthop Res* **28**, 937–941 (2010).
30. Corthesy B, Kao PN. Purification by DNA affinity chromatography of two polypeptides that contact the NF-AT DNA binding site in the interleukin 2 promoter. *J Biol Chem* **269**, 20682–20690 (1994).
31. Shi L, *et al.* Dynamic binding of Ku80, Ku70 and NF90 to the IL-2 promoter in vivo in activated T-cells. *Nucleic Acids Res* **35**, 2302–2310 (2007).
32. Shi L, Godfrey WR, Lin J, Zhao G, Kao PN. NF90 regulates inducible IL-2 gene expression in T cells. *J Exp Med* **204**, 971–977 (2007).
33. Nakadai T, Fukuda A, Shimada M, Nishimura K, Hisatake K. The RNA binding complexes NF45-NF90 and NF45-NF110 associate dynamically with the c-fos gene and function as transcriptional coactivators. *J Biol Chem* **290**, 26832–26845 (2015).
34. Reichman TW, *et al.* Selective regulation of gene expression by nuclear factor 110, a member of the NF90 family of double-stranded RNA-binding proteins. *J Mol Biol* **332**, 85–98 (2003).
35. Wu TH, *et al.* NF90/ILF3 is a transcription factor that promotes proliferation over differentiation by hierarchical regulation in K562 erythroleukemia cells. *PLoS One* **13**, e0193126 (2018).

Figures

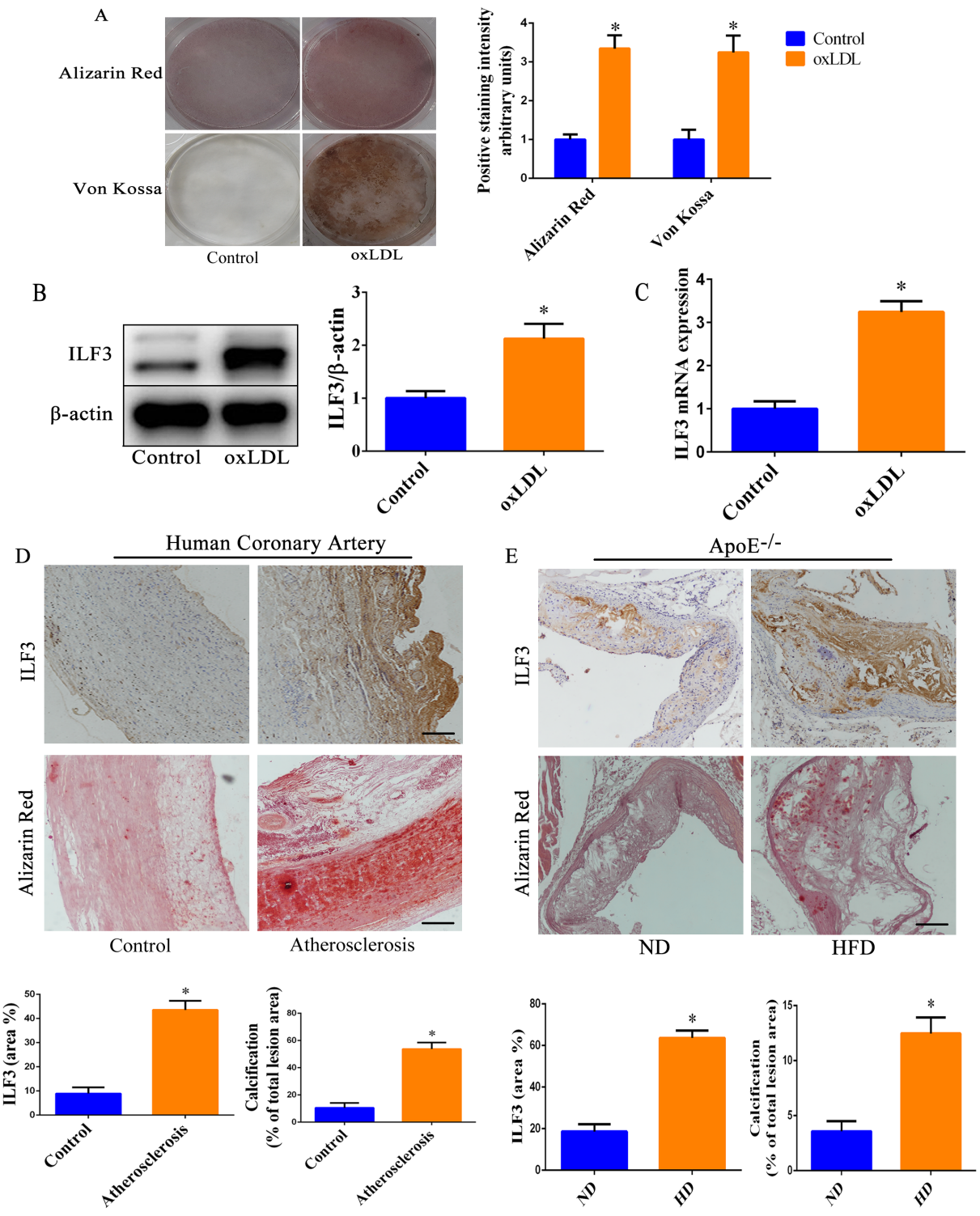

Figure 1

ILF3 is upregulated in hyperlipidemia-induced calcified vascular smooth muscle cells (VSMCs) and atherosclerotic plaque. a HAVSMCs were incubated in osteogenic medium with or without ox-LDL (50μg/ml) for 21 days. Calcification was detected by Alizarin-red and Von Kossa staining (n =5 per

group).*P<0.05, vs. control in osteogenic medium without ox-LDL. b, c Immunoblots and qRT-PCR analyses of the effect of ox-LDL on expression in HAVSMCs (n=5 per group). *P<0.05, vs. control. D Representative immunohistochemical staining of ILF3 and Alizarin-red staining in arteries of healthy control and atherosclerosis mice (n=6 per group, Scale bar: 100μm).*P<0.05, vs. healthy control. e Representative immunohistochemical staining of ILF3 and Alizarin-red staining in atherosclerotic lesions of ApoE-/- mice fed a normal diet (ND) or high fat diet (HFD) for 16 weeks (n=10 per group, Scale bar: 50μm). *P<0.05, vs. ApoE-/- mice fed a normal diet. Data are mean ± SEM (n=5 per group).

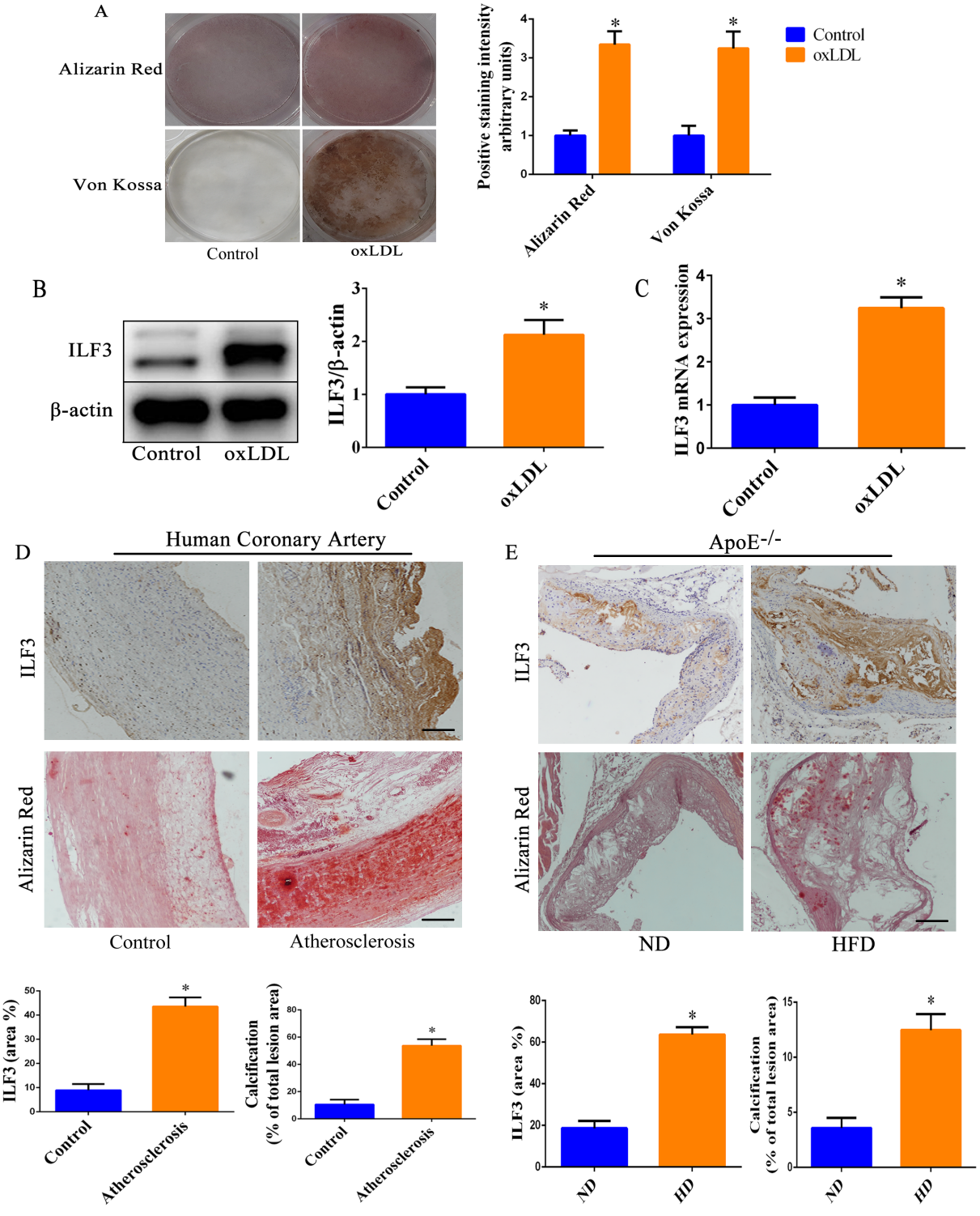

Figure 1

ILF3 is upregulated in hyperlipidemia-induced calcified vascular smooth muscle cells (VSMCs) and atherosclerotic plaque. a HAVSMCs were incubated in osteogenic medium with or without ox-LDL (50μg/ml) for 21 days. Calcification was detected by Alizarin-red and Von Kossa staining (n =5 per group).*P<0.05, vs. control in osteogenic medium without ox-LDL. b, c Immunoblots and qRT-PCR analyses of the effect of ox-LDL on expression in HAVSMCs (n=5 per group). *P<0.05, vs. control. D Representative immunohistochemical staining of ILF3 and Alizarin-red staining in arteries of healthy control and atherosclerosis mice (n=6 per group, Scale bar: 100μm).*P<0.05, vs. healthy control. e Representative immunohistochemical staining of ILF3 and Alizarin-red staining in atherosclerotic lesions of ApoE-/- mice fed a normal diet (ND) or high fat diet (HFD) for 16 weeks (n=10 per group, Scale bar: 50μm). *P<0.05, vs. ApoE-/- mice fed a normal diet. Data are mean ± SEM (n=5 per group).

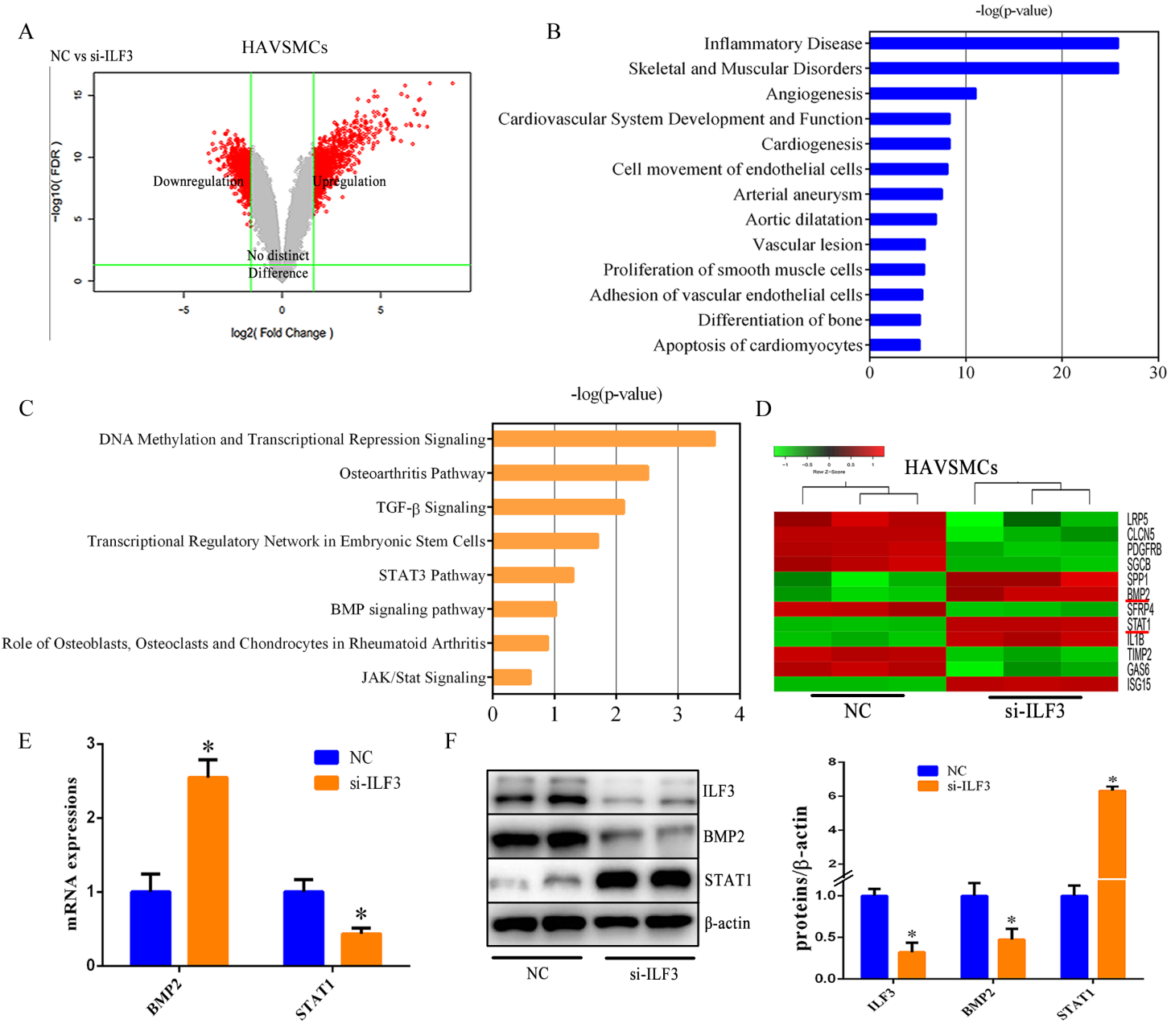

Figure 2

ILF3 participates in regulating transcription of osteogenic-related genes. a Volcano plot of genome-wide transcriptomic analysis shows the differentially expressed genes (DEGs) between normal control (NC) and siRNA-deleted ILF3 (si-ILF3)HAVSMCs. Red points were screened according to the standard of |fold change|≥ 3.0 and false discovery rate <0.05 (n=3 per group) and represent significantly different genes. b and c Gene Ontology analysis of biological processes, molecular functions and cellular components for DEGs related to vascular disease and KEGG pathway analysis of calcification-related classical pathway analysis. The x-axis represents the significance of different terms with negative log10 (P-values). The y-axis shows the name of related terms. ILF3-related diseases and function analysis (b) and ILF3-related classical pathway analysis (c). d HAVSMCs were transfected with si-ILF3 versus negative control (NC). Heatmap shows detailed information of upregulated and downregulated genes for the top induced genes involved in osteoblastic differentiation. Color scale is based on normalized read counts. e HAVSMCs were transfected with negative control siNC or si-ILF3. RT-PCR shows BMP2 and STAT1 mRNA levels in HAVSMCs (n=3 per group). f Representative immunoblot assay of ILF3, BMP2 and STAT1 protein levels in HAVSMCs (n=3 per group) transfected with siNC or si-ILF3. Data are mean ± SEM. *P<0.05 vs NC.

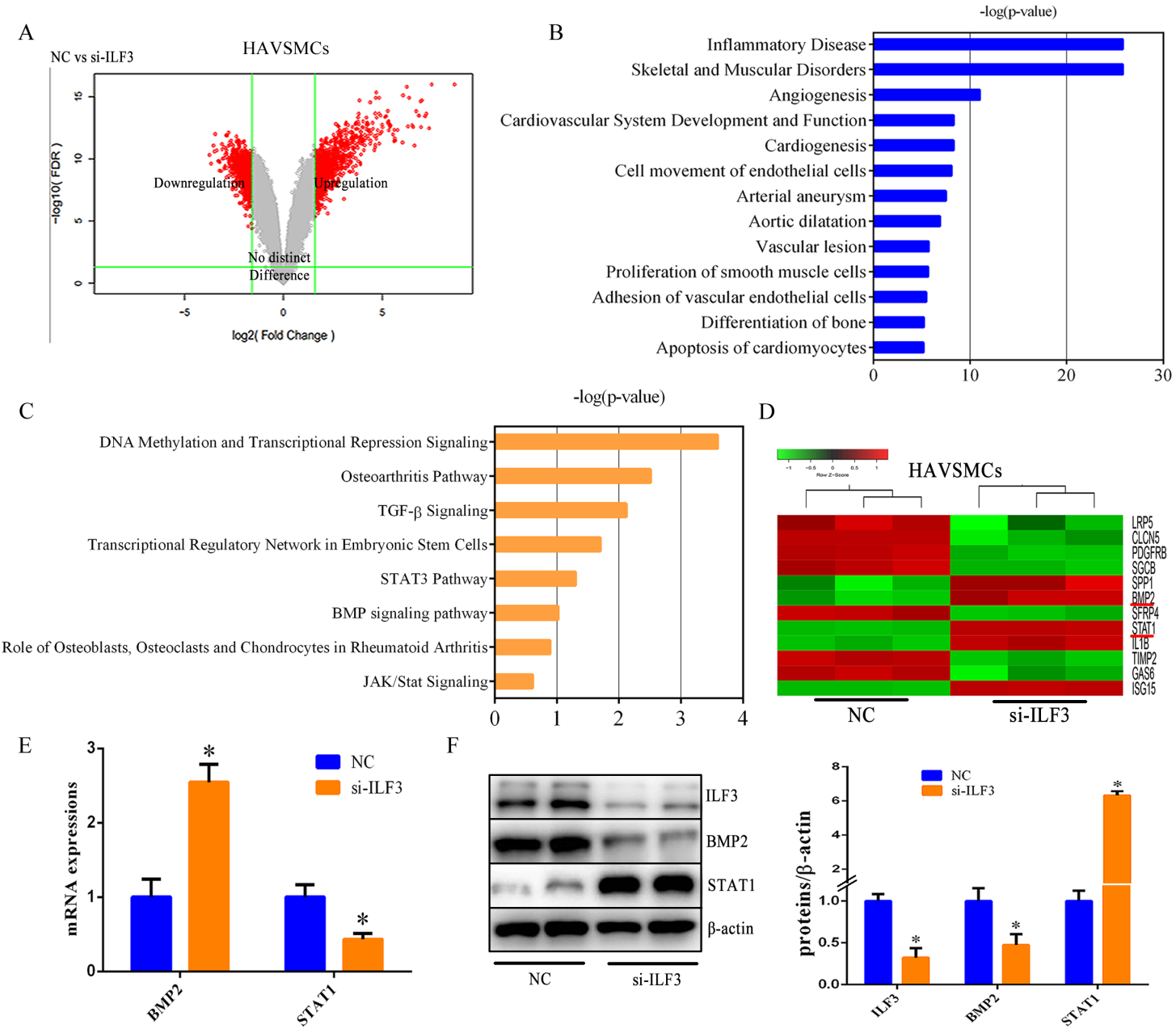

Figure 2

ILF3 participates in regulating transcription of osteogenic-related genes. a Volcano plot of genome-wide transcriptomic analysis shows the differentially expressed genes (DEGs) between normal control (NC) and siRNA-deleted ILF3 (si-ILF3)HAVSMCs. Red points were screened according to the standard of |fold change|≥ 3.0 and false discovery rate <0.05 (n=3 per group) and represent significantly different genes. b and c Gene Ontology analysis of biological processes, molecular functions and cellular components for DEGs related to vascular disease and KEGG pathway analysis of calcification-related classical pathway analysis. The x-axis represents the significance of different terms with negative log10 (P-values). The y-axis shows the name of related terms. ILF3-related diseases and function analysis (b) and ILF3-related classical pathway analysis (c). d HAVSMCs were transfected with si-ILF3 versus negative control (NC).

Heatmap shows detailed information of upregulated and downregulated genes for the top induced genes involved in osteoblastic differentiation. Color scale is based on normalized read counts. e HAVSMCs were transfected with negative control siNC or si-ILF3. RT-PCR shows BMP2 and STAT1 mRNA levels in HAVSMCs (n=3 per group). f Representative immunoblot assay of ILF3, BMP2 and STAT1 protein levels in HAVSMCs (n=3 per group) transfected with siNC or si-ILF3. Data are mean ± SEM. *P<0.05 vs NC.

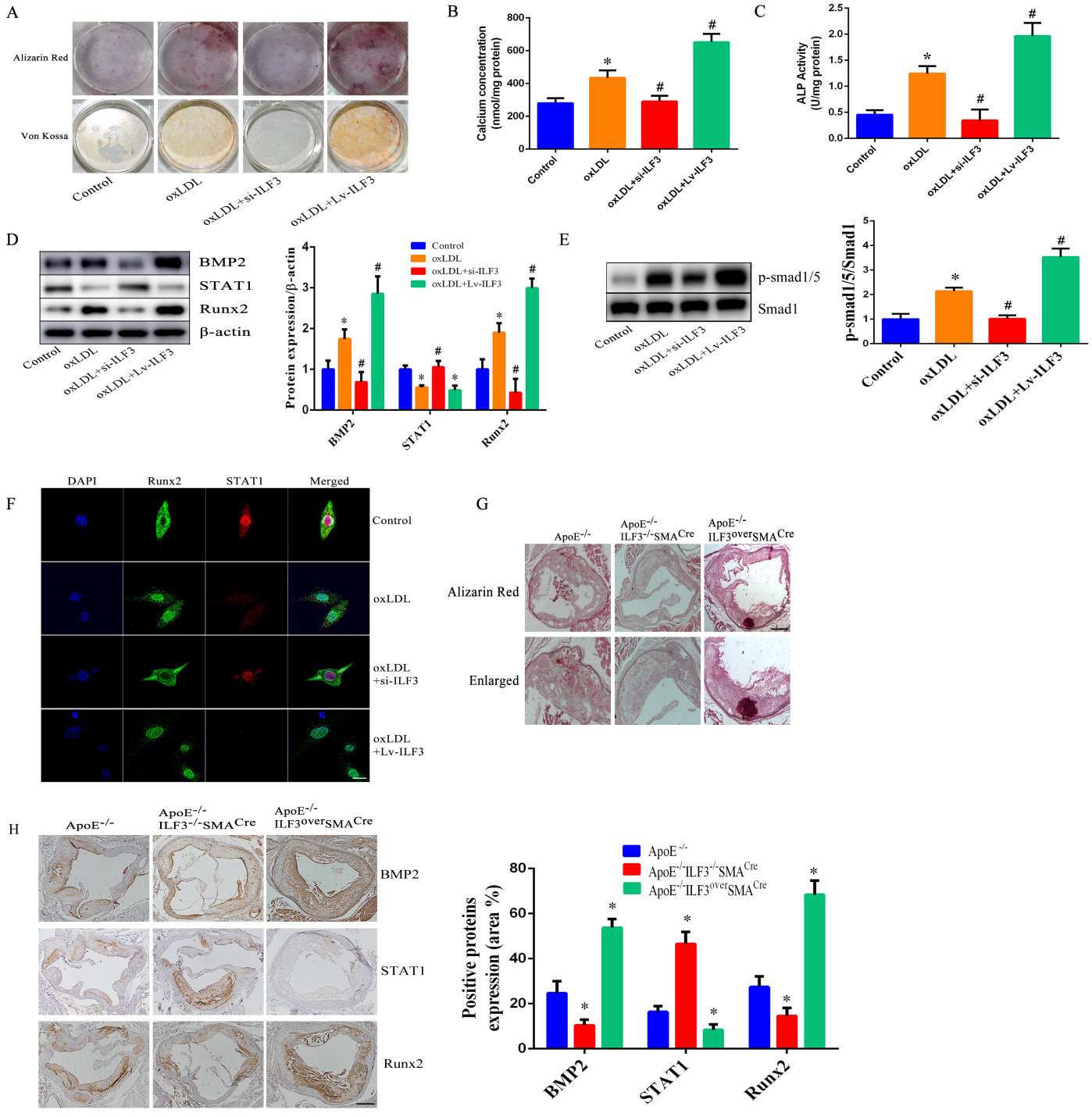

Figure 3

ILF3 promotes hyperlipidemia-induced VSMC calcification in vitro and in vivo. a-f HAVSMCs were transfected with si-ILF3 or lentivirus overexpressing ILF3 (Lv-ILF3), then cultured in osteogenic medium and treated with or without ox-LDL (n=3 per group). a Representative Alizarin-red and Von Kossa staining after treatment with ox-LDL for 14 days. b and c Calcium content and ALP activity in calcified HAVSMCs. Western blot analysis of BMP2, STAT1 and Runx2 protein levels (d) and p-smad1/5 and Smad1 levels (e) and quantification. f Immunofluorescence double staining for Runx2 (green) and STAT1(red) in HAVSMCs. Nuclei were stained with DAPI (blue) (Scale bar: 20 μm).*P<0.05, vs. control in osteogenic medium without ox-LDL and #P<0.05, vs. oxLDL. g Representative Alizarin-red staining in atherosclerotic lesions of ApoE-/-, ApoE-/-ILF3-/-SMACre and ApoE-/-ILF3overSMACre mice fed an HFD for 16 weeks (n=10 per group, Scale bar: 100μm). h Representative immunohistochemical staining and quantification of BMP2, STAT1 and Runx2 levels in atherosclerotic lesions of ApoE-/-, ApoE-/-ILF3-/-SMACre and ApoE-/-ILF3overSMACre mice fed an HFD for 16 weeks (n=10 per group, Scale bar: 100μm).*P<0.05, vs. ApoE-/-mice. Data are mean ± SEM.

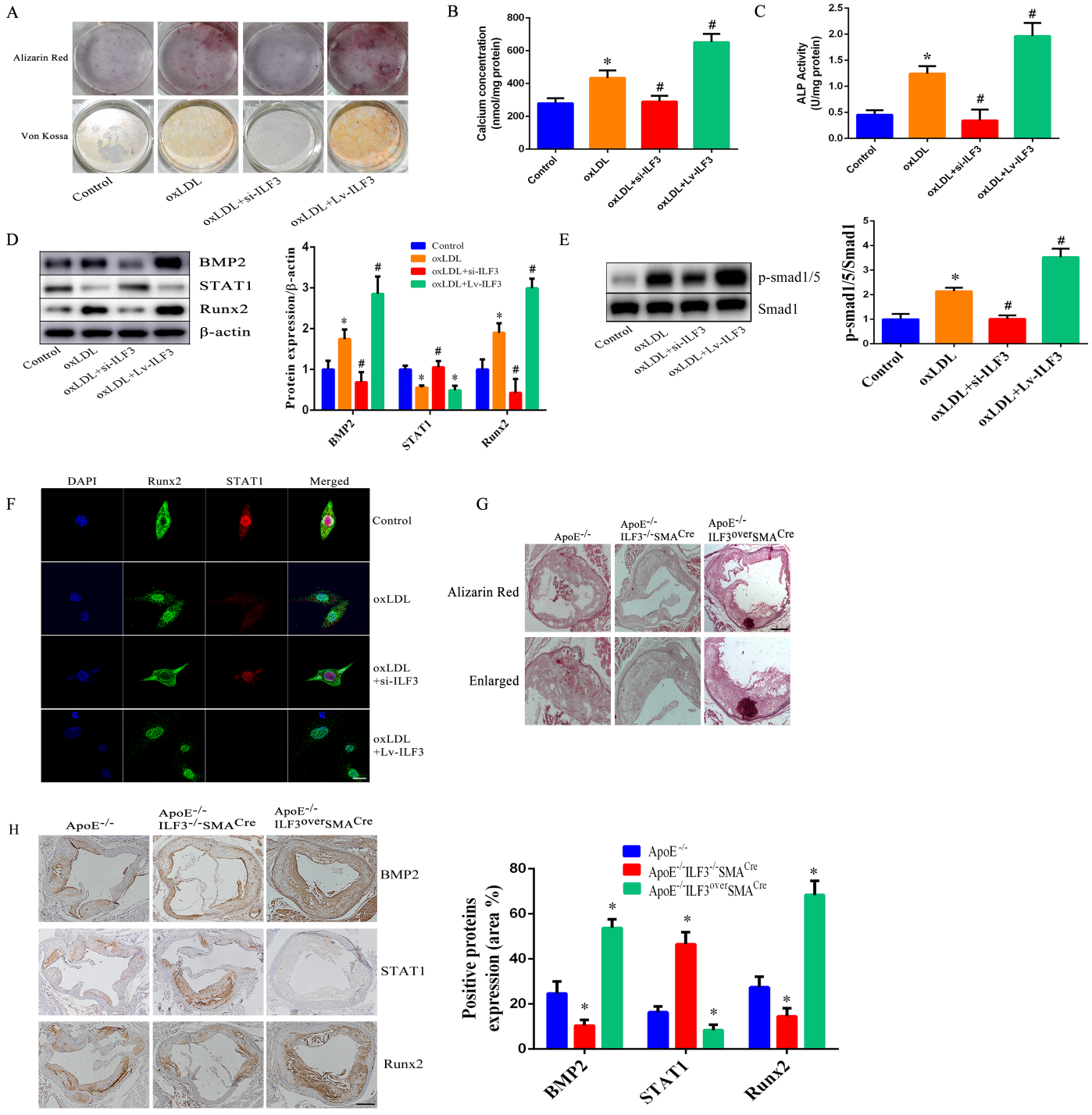

Figure 3

ILF3 promotes hyperlipidemia-induced VSMC calcification in vitro and in vivo. a-f HAVSMCs were transfected with si-ILF3 or lentivirus overexpressing ILF3 (Lv-ILF3), then cultured in osteogenic medium and treated with or without ox-LDL (n=3 per group). a Representative Alizarin-red and Von Kossa staining after treatment with ox-LDL for 14 days. b and c Calcium content and ALP activity in calcified HAVSMCs. Western blot analysis of BMP2, STAT1 and Runx2 protein levels (d) and p-smad1/5 and Smad1 levels (e) and quantification. f Immunofluorescence double staining for Runx2 (green) and STAT1(red) in

HAVSMCs. Nuclei were stained with DAPI (blue) (Scale bar: 20 μm).*P<0.05, vs. control in osteogenic medium without ox-LDL and #P<0.05, vs. oxLDL. g Representative Alizarin-red staining in atherosclerotic lesions of ApoE-/-, ApoE-/-ILF3-/-SMACre and ApoE-/-ILF3overSMACre mice fed an HFD for 16 weeks (n=10 per group, Scale bar: 100μm). h Representative immunohistochemical staining and quantification of BMP2, STAT1 and Runx2 levels in atherosclerotic lesions of ApoE-/-, ApoE-/-ILF3-/-SMACre and ApoE-/-ILF3overSMACre mice fed an HFD for 16 weeks (n=10 per group, Scale bar: 100μm).*P<0.05, vs. ApoE-/-mice. Data are mean ± SEM.

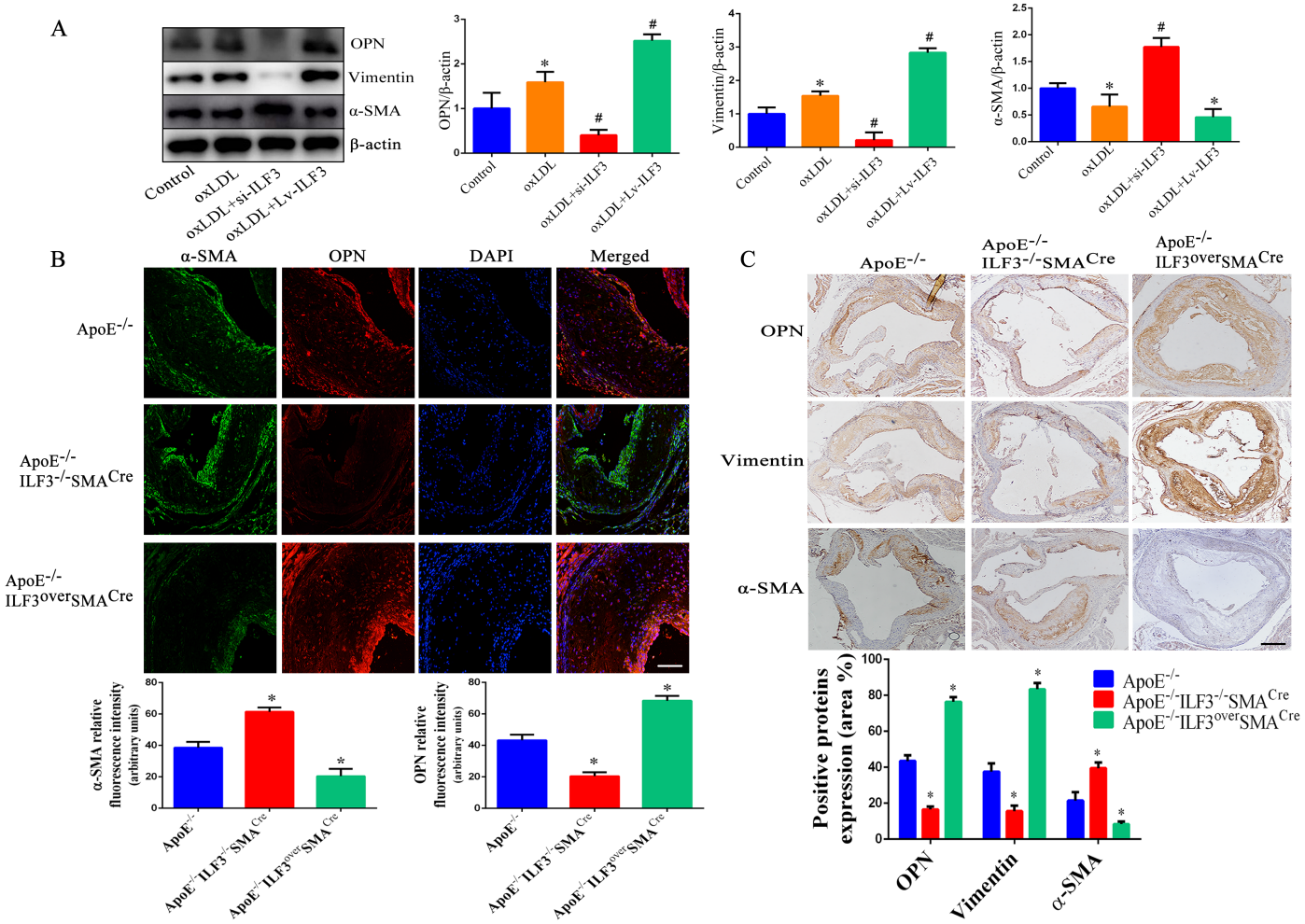

Figure 4

ILF3 mediated hyperlipidemia-induced VSMC synthetic phenotype switch. a Western blot analysis of synthetic (OPN, Vimentin) and contractile (α-SMA) protein levels and quantification in HAVSMCs cultured in osteogenic medium and treated with or without ox-LDL (n=3 per group). *P<0.05, vs. control and #P<0.05, vs. ox-LDL. b Immunofluorescence double staining for α-SMA (green) and OPN (red) in atherosclerotic lesions of ApoE-/-, ApoE-/-ILF3-/-SMACre and ApoE-/-ILF3overSMACre mice fed a HFD for 16 weeks (n=10 per group, Scale bar: 50μm). c Immunohistochemical staining for α-SMA, OPN and Vimentin (n=10 per group, Scale bar: 100μm).*P<0.05, vs. ApoE-/-mice. Data are mean ± SEM.

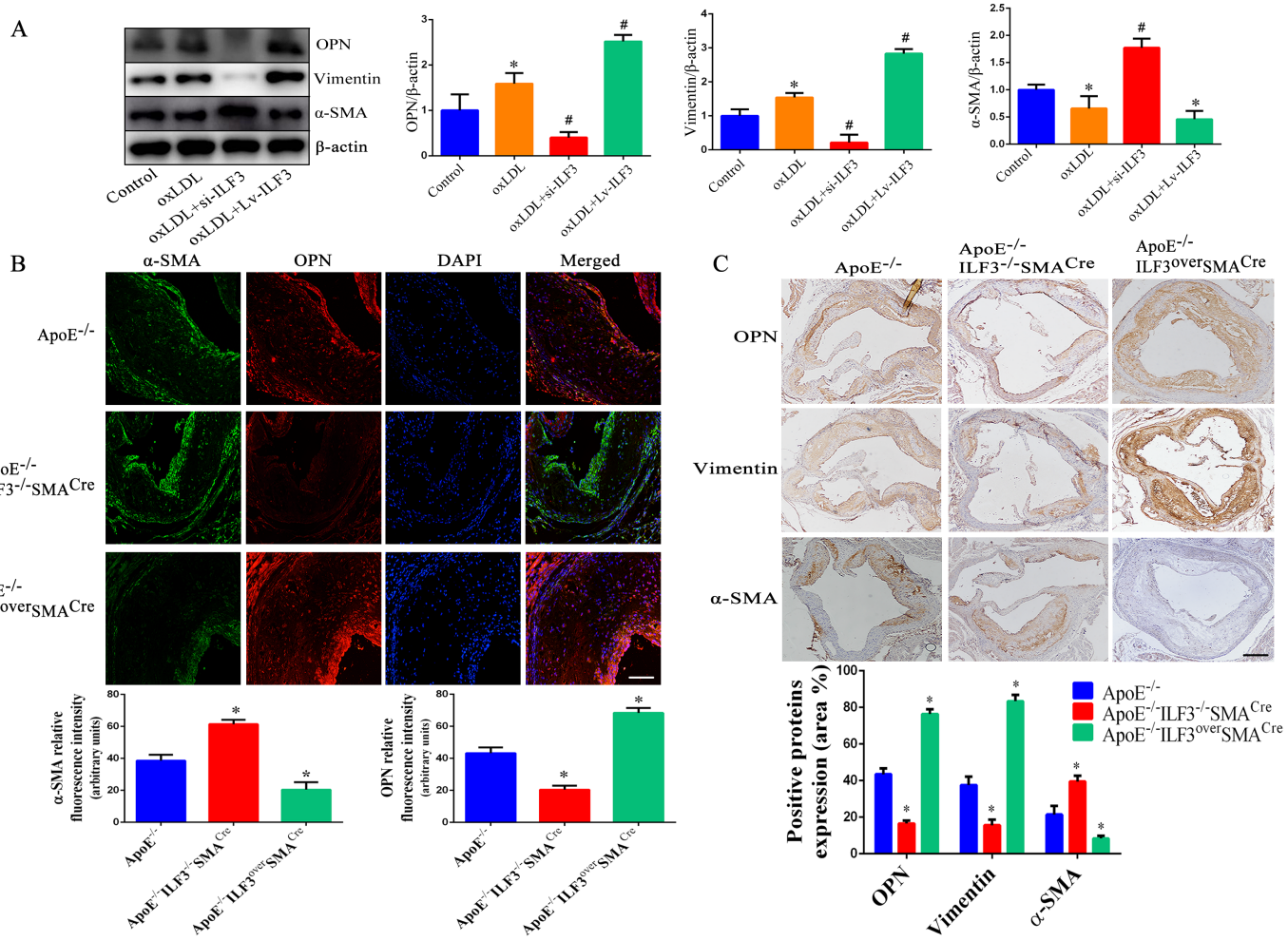

Figure 4

ILF3 mediated hyperlipidemia-induced VSMC synthetic phenotype switch. a Western blot analysis of synthetic (OPN, Vimentin) and contractile (α-SMA) protein levels and quantification in HAVSMCs cultured in osteogenic medium and treated with or without ox-LDL (n=3 per group). *P<0.05, vs. control and #P<0.05, vs. ox-LDL. b Immunofluorescence double staining for α-SMA (green) and OPN (red) in atherosclerotic lesions of ApoE-/-, ApoE-/-ILF3-/-SMACre and ApoE-/-ILF3overSMACre mice fed a HFD for 16 weeks (n=10 per group, Scale bar: 50μm). c Immunohistochemical staining for α-SMA, OPN and Vimentin (n=10 per group, Scale bar: 100μm).*P<0.05, vs. ApoE-/-mice. Data are mean ± SEM.

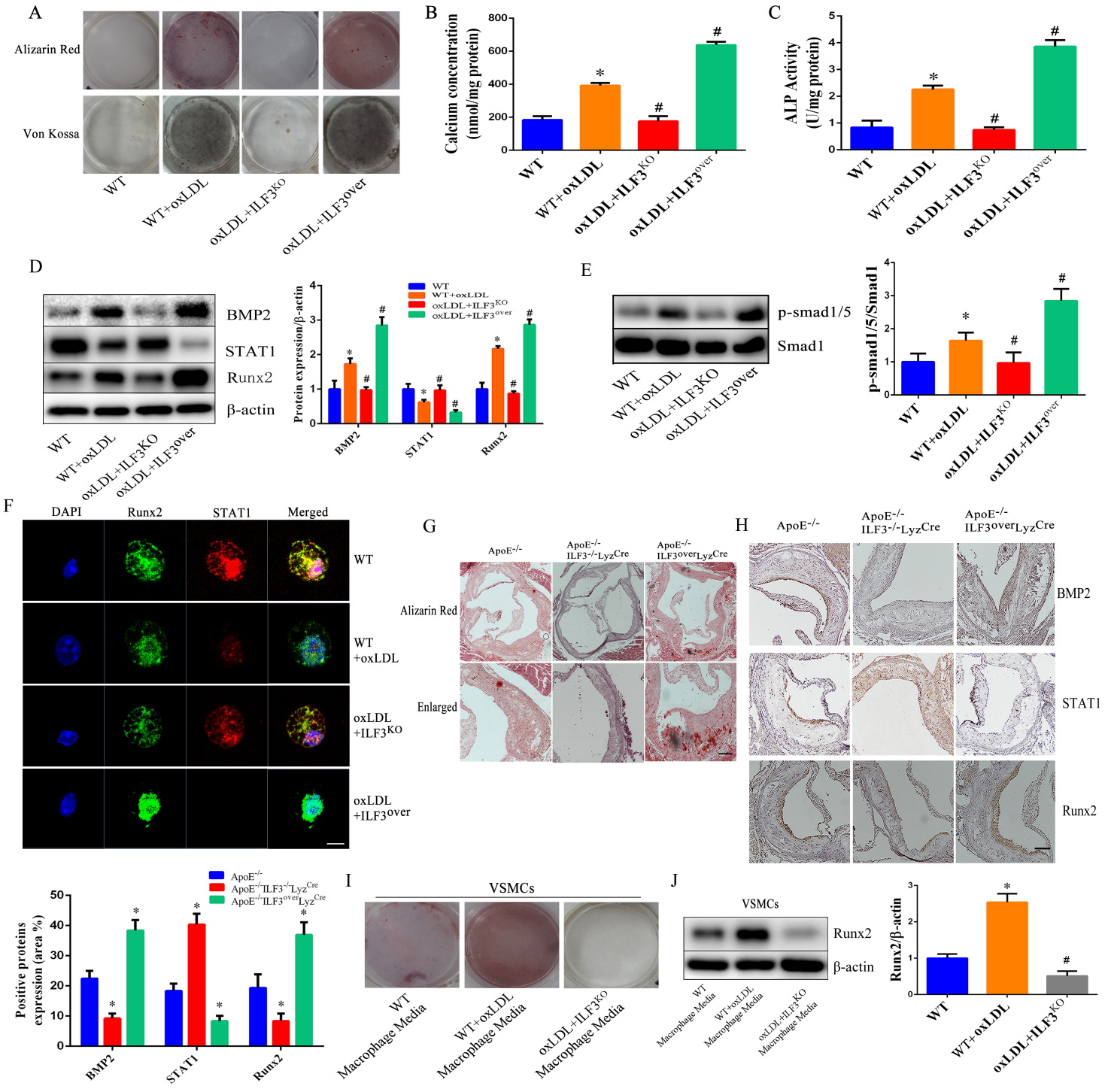

Figure 5

ILF3 accelerates atherosclerotic calcification by inducing macrophage calcification. a-f Primary macrophages from wild type (WT), ILF3-/-/LyzCre and ILF3over/LyzCre mice were incubated with osteogenic medium and with or without ox-LDL (n=3 per group). a Calcification were evaluated by Alizarin-red or von Kossa staining after treatment with ox-LDL for 14 days. b Quantification of calcium content. c Measurement of ALP activity. Western blot analysis of BMP2, STAT1 and Runx2 protein levels (d) in macrophages and p-smad1/5 and Smad1 levels (e) and quantification. f Immunofluorescence

double staining for Runx2 (green) and STAT1 (red) in HAVSMCs. Nuclei were stained with DAPI (blue) (Scale bar: 10μm).*P<0.05, vs. WT and #P<0.05, vs. WT+oxLDL. g Representative Alizarin-red staining in atherosclerotic lesions of ApoE-/-, ApoE-/-ILF3-/-/LyzCre and ApoE-/-ILF3over/LyzCre mice fed a HFD for 16 weeks (n=10 per group, Scale bar: 100μm). h Representative immunohistochemical staining and quantification of BMP2, STAT1 and Runx2 levels in atherosclerotic lesions of ApoE-/-, ApoE-/-ILF3-/-/LyzCre and ApoE-/-ILF3over/LyzCre mice fed a HFD for 16 weeks (n=10 per group, Scale bar: 50μm).*P<0.05, vs. ApoE-/-mice. i and j HAVSMCs showed calcification on stimulation with conditioned medium from WT mouse macrophages for 2 weeks, accompanied by higher levels of Runx2. ILF3 deficiency abolished the pro-calcification effect of macrophages (n=3 per group).*P<0.05, vs. WT and #P<0.05, vs. WT+ox-LDL. Data are mean ± SEM.

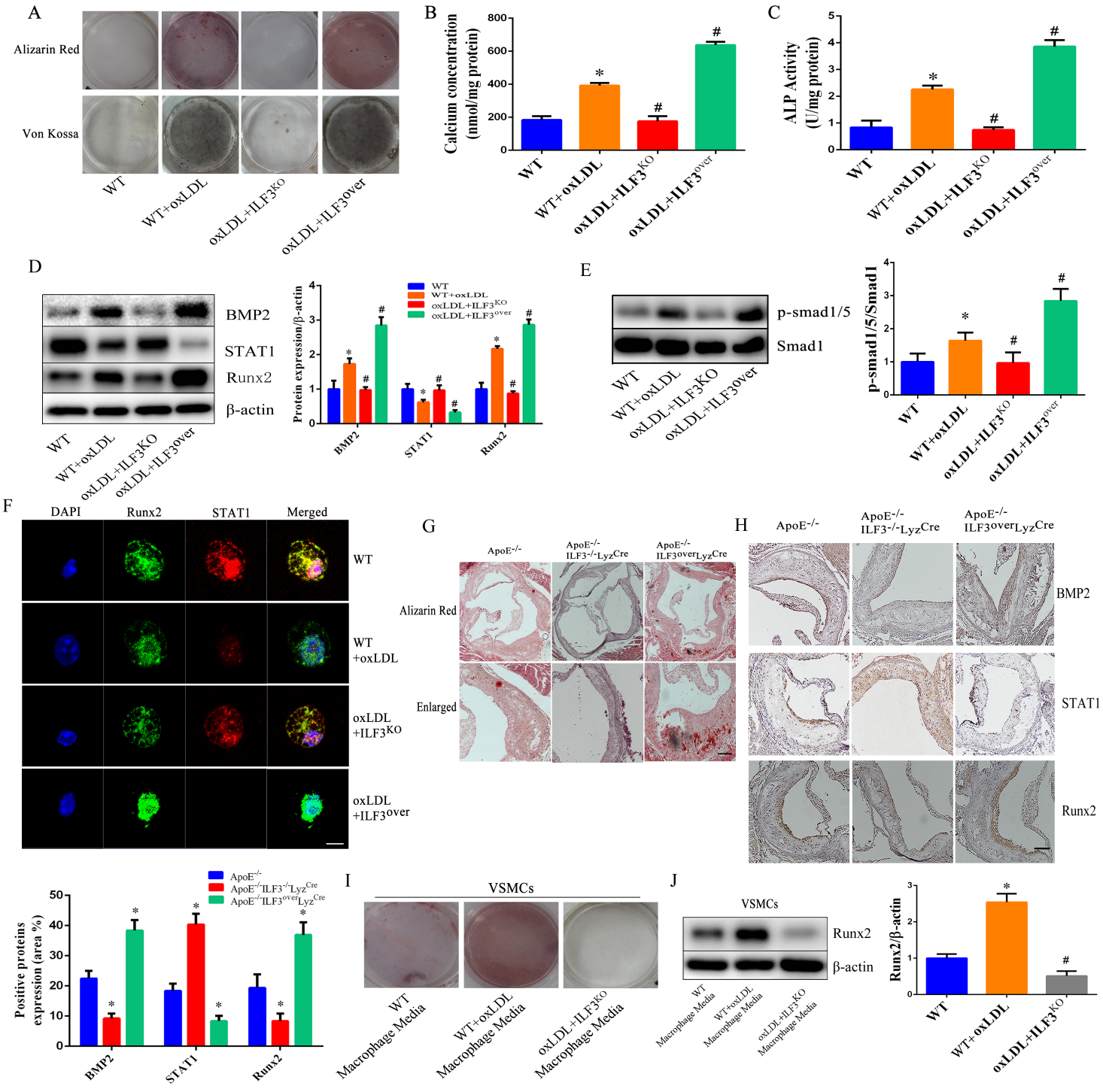

Figure 5

ILF3 accelerates atherosclerotic calcification by inducing macrophage calcification. a-f Primary macrophages from wild type (WT), ILF3-/-/LyzCre and ILF3over/LyzCre mice were incubated with osteogenic medium and with or without ox-LDL (n=3 per group). a Calcification were evaluated by Alizarin-red or von Kossa staining after treatment with ox-LDL for 14 days. b Quantification of calcium content. c Measurement of ALP activity. Western blot analysis of BMP2, STAT1 and Runx2 protein levels (d) in macrophages and p-smad1/5 and Smad1 levels (e) and quantification. f Immunofluorescence

double staining for Runx2 (green) and STAT1 (red) in HAVSMCs. Nuclei were stained with DAPI (blue) (Scale bar: 10μm).*P<0.05, vs. WT and #P<0.05, vs. WT+oxLDL. g Representative Alizarin-red staining in atherosclerotic lesions of ApoE-/-, ApoE-/-ILF3-/-/LyzCre and ApoE-/-ILF3over/LyzCre mice fed a HFD for 16 weeks (n=10 per group, Scale bar: 100μm). h Representative immunohistochemical staining and quantification of BMP2, STAT1 and Runx2 levels in atherosclerotic lesions of ApoE-/-, ApoE-/-ILF3-/-/LyzCre and ApoE-/-ILF3over/LyzCre mice fed a HFD for 16 weeks (n=10 per group, Scale bar: 50μm).*P<0.05, vs. ApoE-/-mice. i and j HAVSMCs showed calcification on stimulation with conditioned medium from WT mouse macrophages for 2 weeks, accompanied by higher levels of Runx2. ILF3 deficiency abolished the pro-calcification effect of macrophages (n=3 per group).*P<0.05, vs. WT and #P<0.05, vs. WT+ox-LDL. Data are mean ± SEM.

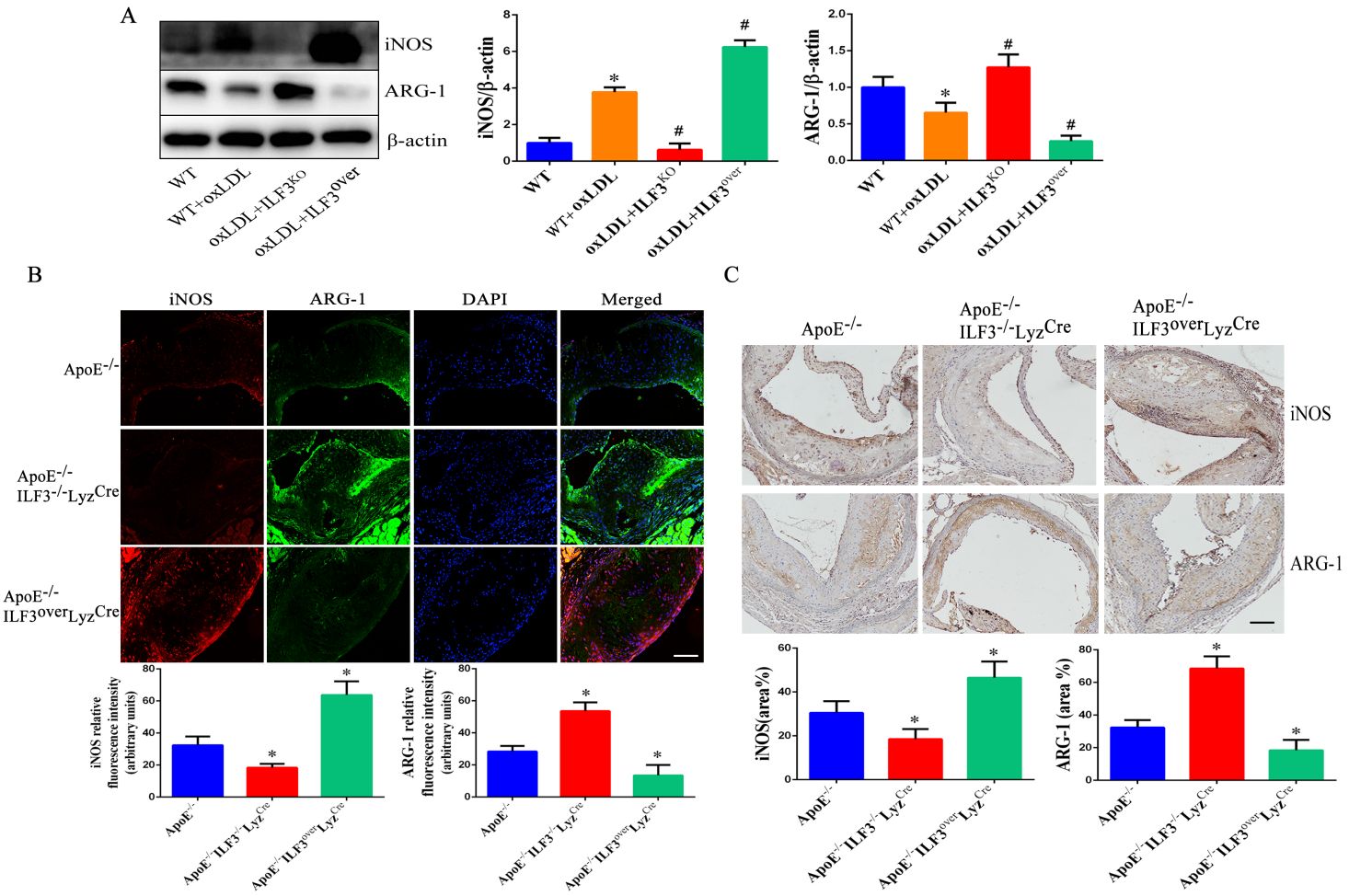

Figure 6

ILF3 enhances atherosclerotic calcification by mediating macrophage polarization. a Western blot analysis of iNOS (marker of M1 macrophage) and ARG1 (marker of M2 macrophage) levels and quantification in primary macrophages from wild type (WT), ILF3-/-/LyzCre and ILF3over/LyzCre mice cultured in osteogenic medium with or without ox-LDL for 3 days (n=3 per group). *P<0.05, vs. WT and #P<0.05, vs. WT+oxLDL. b Representative immunofluorescence double staining and quantification of iNOS (red) and ARG1 (green) in atherosclerotic lesions of ApoE-/-, ApoE-/-ILF3-/-/LyzCre and ApoE-/-

ILF3over/LyzCre mice fed a HFD for 16 weeks (n=10 per group, Scale bar: 50μm). c Representative immunohistochemical staining of iNOS and ARG1 (n=10 per group, Scale bar: 50μm). *P<0.05, vs. ApoE-/-. Data are mean ± SEM.

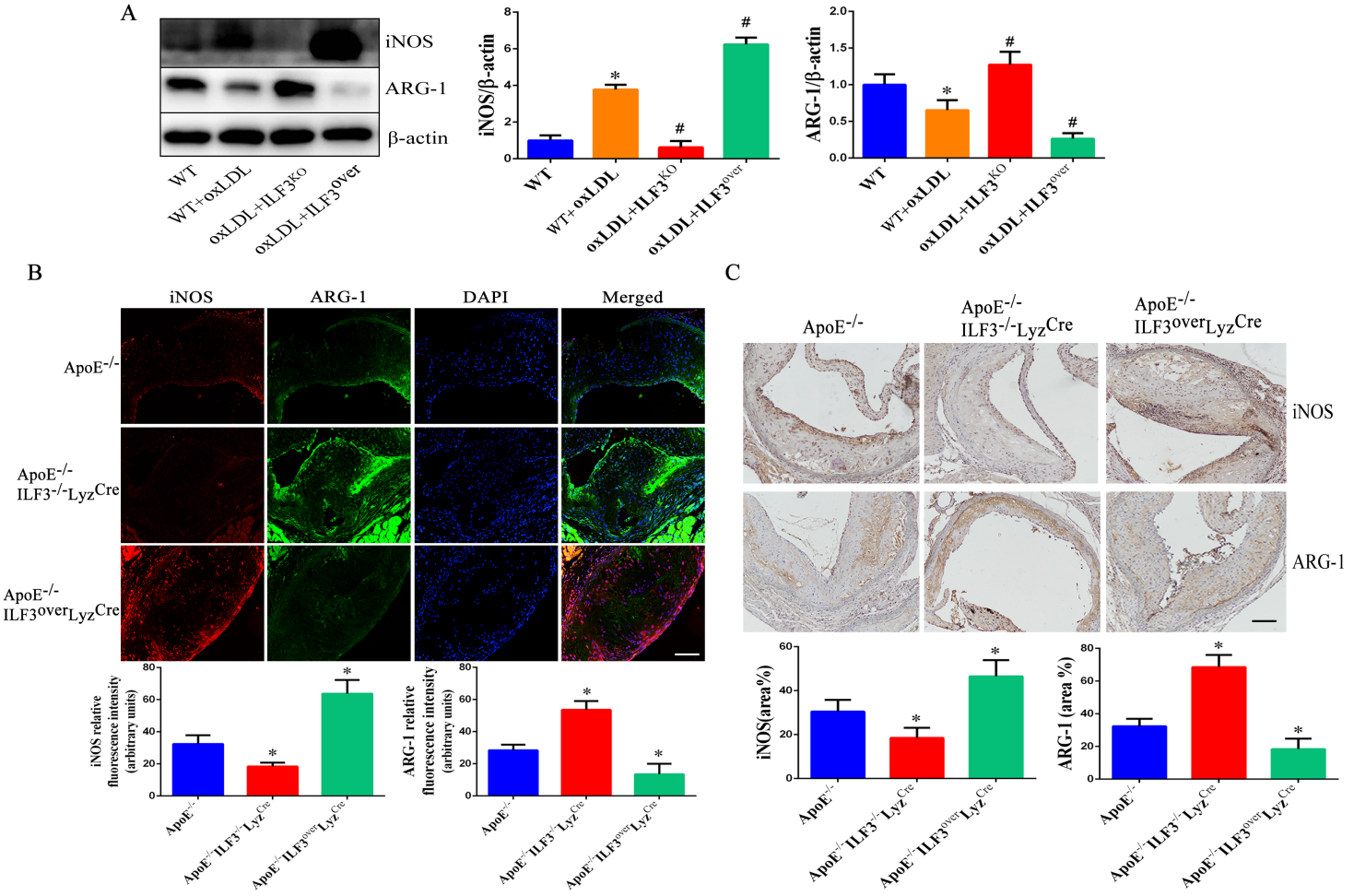

Figure 6

ILF3 enhances atherosclerotic calcification by mediating macrophage polarization. a Western blot analysis of iNOS (marker of M1 macrophage) and ARG1 (marker of M2 macrophage) levels and quantification in primary macrophages from wild type (WT), ILF3-/-/LyzCre and ILF3over/LyzCre mice cultured in osteogenic medium with or without ox-LDL for 3 days (n=3 per group). *P<0.05, vs. WT and #P<0.05, vs. WT+oxLDL. b Representative immunofluorescence double staining and quantification of iNOS (red) and ARG1 (green) in atherosclerotic lesions of ApoE-/-, ApoE-/-ILF3-/-/LyzCre and ApoE-/-ILF3over/LyzCre mice fed a HFD for 16 weeks (n=10 per group, Scale bar: 50μm). c Representative immunohistochemical staining of iNOS and ARG1 (n=10 per group, Scale bar: 50μm). *P<0.05, vs. ApoE-/-. Data are mean ± SEM.

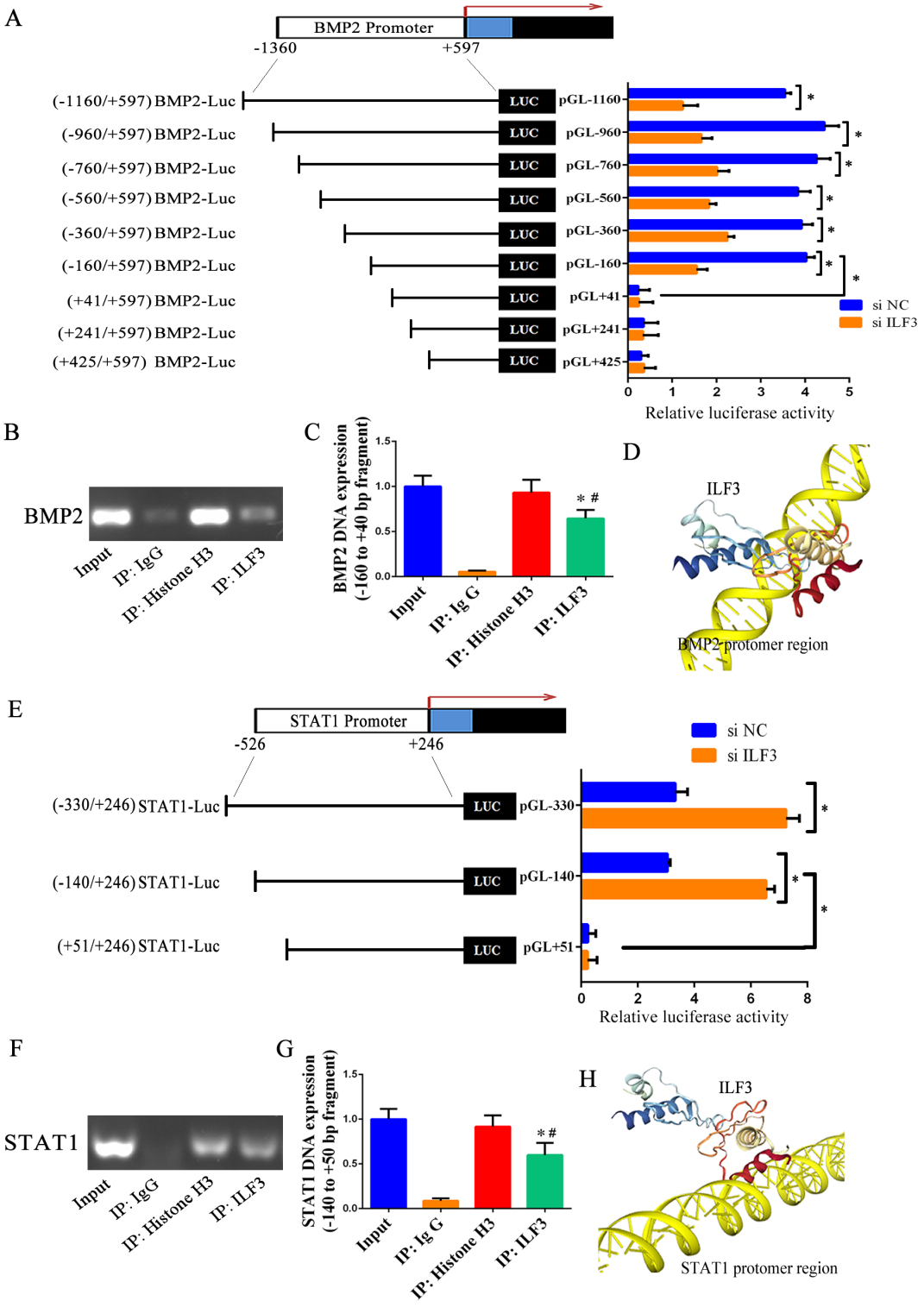

Figure 7

ILF3 binds to the BMP2 and STAT1 promoter regions and contributes to arteriosclerotic calcification. a Relative luciferase activity assay of HEK293T cells after transfection with pGL3-promoter constructs containing DNA fragments serially deleted from -1160 to +597 bp of the promoter BMP2 (n=5 per group). *P<0.05, vs. transfection with negative control siRNA (siNC) or pGL-160. b ChIP assay to verify binding of ILF3 to the BMP2 promoter (n=3 per group). c qPCR analysis of DNA level of BMP2 promoter containing

-160 to +40 bp (n=3 per group). *P<0.05, vs. IgG and #P<0.05, vs. Histone H3. d HADDOCK software was used to evaluate the spatial structure of ILF3-BMP2 promoter regions, and ILF3 binding sites were identified as the AGGGAG site (-53 to -48 bp) in the BMP2 promoter. e Luciferase activity assay after transfection with the STAT1 promoter serially deleted from -526 to +246 bp in HEK293T cells (n=5 per group). *P<0.05, vs. transfection with siNC or pGL-140. f ChIP assay to confirm binding of ILF3 to the STAT1 promoter (n=3 per group). g qPCR of DNA level of STAT1 promoter containing -140 to +50 bp (n=3 per group). *P<0.05, vs. IgG and #P<0.05, vs. Histone H3. h HADDOCK software analysis to evaluate spatial structure of ILF3-STAT1 promoter regions and ILF3 binding sites identified as the GCGCCC site (-28 to -23 bp) of STAT1 promoter. Data are mean ± SEM.

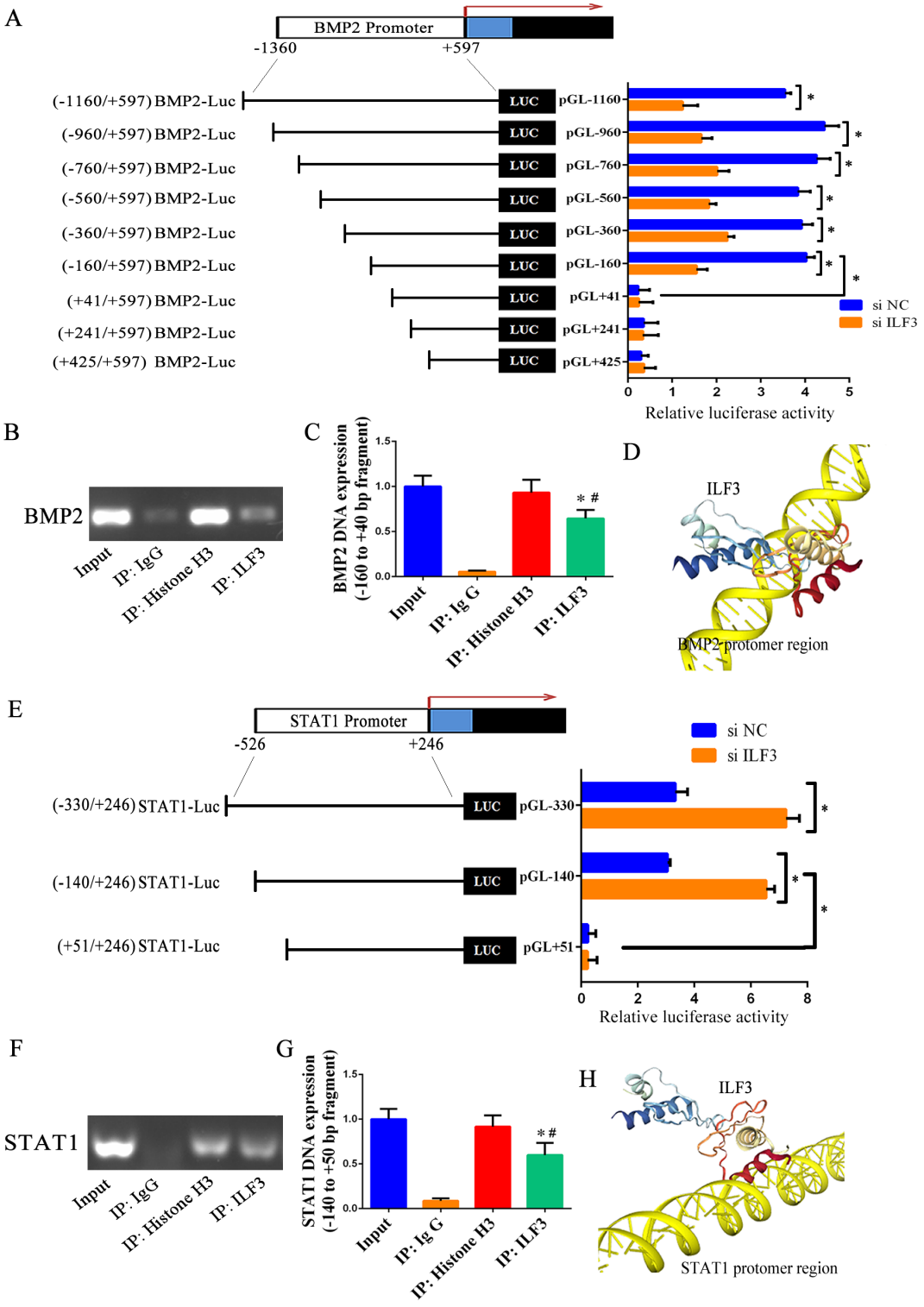

Figure 7

ILF3 binds to the BMP2 and STAT1 promoter regions and contributes to arteriosclerotic calcification. a Relative luciferase activity assay of HEK293T cells after transfection with pGL3-promoter constructs containing DNA fragments serially deleted from -1160 to +597 bp of the promoter BMP2 (n=5 per group). *P<0.05, vs. transfection with negative control siRNA (siNC) or pGL-160. b ChIP assay to verify binding of ILF3 to the BMP2 promoter (n=3 per group). c qPCR analysis of DNA level of BMP2 promoter containing

-160 to +40 bp (n=3 per group). *P<0.05, vs. IgG and #P<0.05, vs. Histone H3. d HADDOCK software was used to evaluate the spatial structure of ILF3-BMP2 promoter regions, and ILF3 binding sites were identified as the AGGGAG site (-53 to -48 bp) in the BMP2 promoter. e Luciferase activity assay after transfection with the STAT1 promoter serially deleted from -526 to +246 bp in HEK293T cells (n=5 per group). *P<0.05, vs. transfection with siNC or pGL-140. f ChIP assay to confirm binding of ILF3 to the STAT1 promoter (n=3 per group). g qPCR of DNA level of STAT1 promoter containing -140 to +50 bp (n=3 per group). *P<0.05, vs. IgG and #P<0.05, vs. Histone H3. h HADDOCK software analysis to evaluate spatial structure of ILF3-STAT1 promoter regions and ILF3 binding sites identified as the GCGCCC site (-28 to -23 bp) of STAT1 promoter. Data are mean ± SEM.

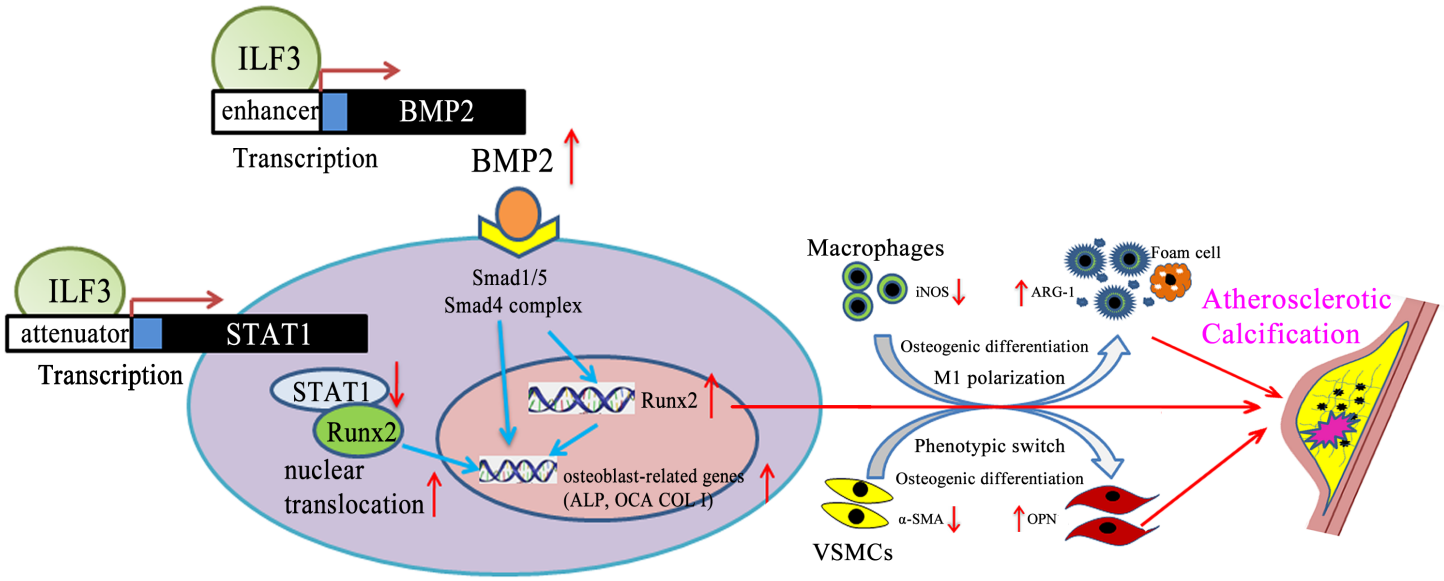

Figure 8

Schematic diagram of ILF3 promoting atherosclerotic calcification ILF3 functions as an indirect regulator of Runx2 expression by targeting BMP2 and STAT1 transcription. The increase in BMP2 level and decrease in STAT1 level induces Runx2 expression and function, which results in an osteogenic switch of both VSMCs and macrophages. VSMCs undergo a phenotype alteration from a contractile to dedifferentiated synthetic phenotype, and macrophages transform from an anti-inflammatory M2 to pro-inflammatory M1 phenotype. So, ILF3 accelerates the osteogenic differentiation of both VSMCs and macrophages and further promotes atherosclerotic calcification by acting on the regulation of BMP2 and STAT1 transcription levels.

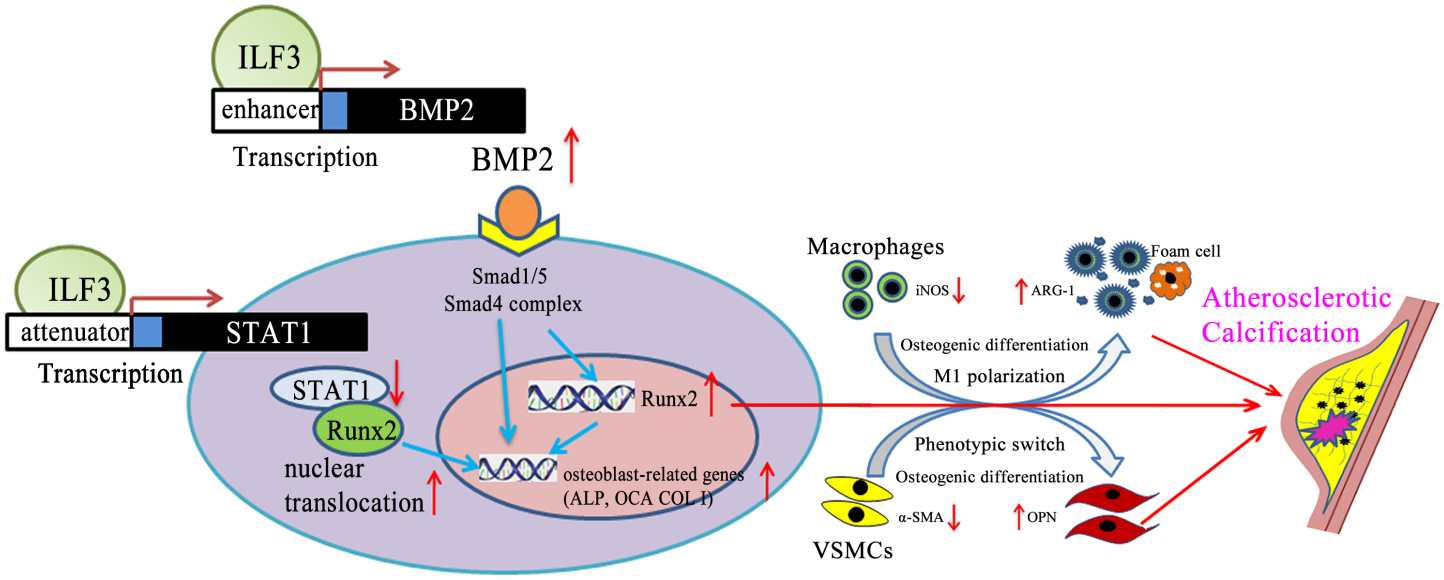

Figure 8

Schematic diagram of ILF3 promoting atherosclerotic calcification ILF3 functions as an indirect regulator of Runx2 expression by targeting BMP2 and STAT1 transcription. The increase in BMP2 level and decrease in STAT1 level induces Runx2 expression and function, which results in an osteogenic switch of both VSMCs and macrophages. VSMCs undergo a phenotype alteration from a contractile to dedifferentiated synthetic phenotype, and macrophages transform from an anti-inflammatory M2 to pro-inflammatory M1 phenotype. So, ILF3 accelerates the osteogenic differentiation of both VSMCs and macrophages and further promotes atherosclerotic calcification by acting on the regulation of BMP2 and STAT1 transcription levels.

Supplementary Files

This is a list of supplementary files associated with this preprint. Click to download.

- Table.1.docx
- Table.1.docx
- Table.2.docx
- Table.2.docx
- Table.3.docx
- Table.3.docx